



Article

Mapping Aquifer Recharge Potential Zones (ARPZ) Using Integrated Geospatial and Analytic Hierarchy Process (AHP) in an Arid Region of Saudi Arabia

Mohd Yawar Ali Khan ^{1,*}, Mohamed ElKashouty ¹ , Faisal K. Zaidi ² and Johnbosco C. Egbueri ³

¹ Department of Hydrogeology, Faculty of Earth Sciences, King Abdulaziz University, Jeddah 21589, Saudi Arabia; melkashouty@kau.edu.sa

² Geology and Geophysics Department, College of Science, King Saud University, Riyadh 11451, Saudi Arabia; fzaidi@ksu.edu.sa

³ Department of Geology, Chukwuemeka Odumegwu Ojukwu University, Uli 464104, Nigeria; jc.egbueri@coou.edu.ng

* Correspondence: makhan7@kau.edu.sa

Abstract: There is an urgent need to explore and analyze new aquifer recharge potential zones (ARPZ) in arid regions exposed mainly to hard rock local aquifers, whether fractured or non-fractured, for investment and fulfillment of the Saudi Vision 2030. Over-pumping, seawater intrusion, climatological changes, population growth, lack of traditional water supplies, expensive desalinated water, and excessive evaporation have characterized the Duba region of Tabuk province of Saudi Arabia (SA). Aquifer productivity and potentiality are affected by surface geology, rainfall, lineament density, drainage density, slope, elevation, soil, and normalized difference vegetation index (NDVI). This study aims to demarcate the ARPZ using integrated remote sensing and geographic information system (GIS) and (RS) approaches. The relative importance of each parameter was determined based on its impact on the aquifer's potential through the analytical hierarchical process (AHP). The ARPZ zones are categorized into five classes starting from very low to very high potentiality. Southern, western, and northern areas have high to very high aquifer potentiality and recharge. They made up roughly 43% of the area that was examined. About 41.8% of the research area is comprised of low to very low groundwater potentiality, and this potentiality is dispersed over the western and central regions of the region. The medium aquifer potentiality level reflects about 15.2%. The high to very high aquifer potentiality areas coincide with low concentrations of total dissolved solids (TDS), electrical conductivity (EC), and nitrate (NO₃). The outcomes emphasized the decisiveness of the entire study and its applicability to any place with similar groundwater aspirations and management.

Keywords: groundwater; analytical hierarchical process; remote sensing; ARPZ; Duba; Saudi Arabia



Citation: Khan, M.Y.A.; ElKashouty, M.; Zaidi, F.K.; Egbueri, J.C. Mapping Aquifer Recharge Potential Zones (ARPZ) Using Integrated Geospatial and Analytic Hierarchy Process (AHP) in an Arid Region of Saudi Arabia. *Remote Sens.* **2023**, *15*, 2567. <https://doi.org/10.3390/rs15102567>

Academic Editors: Chuen-Fa Ni and Jiun-Yee Yen

Received: 15 March 2023

Revised: 11 May 2023

Accepted: 12 May 2023

Published: 14 May 2023



Copyright: © 2023 by the authors. Licensee MDPI, Basel, Switzerland. This article is an open access article distributed under the terms and conditions of the Creative Commons Attribution (CC BY) license (<https://creativecommons.org/licenses/by/4.0/>).

1. Introduction

Groundwater is one of the most valuable and scarce subsurface resources, with significant value to human, aquatic, and terrestrial ecosystems [1–3]. Water demand has risen dramatically in recent decades, particularly in arid and semi-arid regions of the world. The ever-increasing demand for water has put tremendous pressure on scarce freshwater resources. A significant increase in freshwater resources is required due to the rising population density, contamination, seawater intrusion, industrialization, agricultural development, high cost of desalinated water, and urbanization [4–13]. Exploration and exploitation of aquifers through geophysics, geology, and hydrogeology are expensive and time-consuming [14]. Occasionally, hydrological, hydrogeological, and geological data are scant or nonexistent. Consequently, it is necessary to determine the ARPZ on a local and regional scale with the optimal pumping rate [15–20]. The ARPZ is the initial step in aquifer management and resource allocation. The aquifer potential area suggests that

the rate of aquifer abstraction was high [21]. Geospatial techniques were applied for data modeling and analysis at the regional level, saving time and money.

Topography, lithology, tectonics, lineaments density, fractures concentration, slope, porosity, permeability, soil types, land use land cover (LULC), and drainage networks all impact the groundwater recharge [22]. The ARPZ was determined using the specified weights for the abovementioned variables based on their contribution to groundwater potentiality. The approaches for extracting aquifer potentiality used RS and GIS. Geographic, hydrogeological, and geological data were distributed using GIS. The LULC, soil types, and fractures are identified using RS techniques. They then switched to GIS for analysis and overlay. The AHP tool was utilized for the delineation of ARPZ [18,23–25]. It manages the outputs and simplifies complex opinions to pair-wise series comparisons. In recent years, GIS techniques have been utilized in conjunction with multi-criteria decision-making (MCDM) technologies, such as the analytic hierarchy process (AHP) [26], to assign weights to thematic layers [27]. These techniques can effectively incorporate structure, suitability, and precision into decision-making [23,28]. The application of AHP techniques in environmental problem-solving and management is now widespread. Numerous scientists have utilized AHP in ecological impact assessments [29–31] and solid waste management [32,33]. The most extensively used and successfully implemented application of AHP technology [34–41] is potential groundwater mapping and locating suitable sites for artificial recharge.

According to the World Bank [42], if appropriate plans are not implemented, freshwater in SA will deteriorate and become a source of concern by 2025. Most aquifers along the Red Seas coast suffered from seawater intrusion due to over-pumping. In many parts of SA, the expansion of agricultural activities contaminates the aquifers with NO_3 pollutants. According to FAO/WHO [43], water consumption in SA grew from $2352 \times 10^6 \text{ m}^3$ in 1980 to more than $20,000 \times 10^6 \text{ m}^3$ in 2004. 88% of it is used for irrigation in agriculture, 9% for domestic purposes, and 3% for industrial requirements. Agriculture wastewater production keeps rising over time. Due to the limited fractures and joints lacking hydrogeologic interconnectedness, most aquifers were composed of hard rocks and represented local rather than regional aquifers. In the northern and eastern regions of SA, sedimentary aquifers are concentrated. High temperatures throughout the year caused the shallow aquifer to evaporate, which raised the groundwater's TDS concentration. The aquifer reserves were determined at $1919 \times 10^9 \text{ m}^3$, of which $160 \times 10^9 \text{ m}^3$ is stored in deeper aquifers [44]. The presence of inorganic contaminants from rock–water interaction (desorption) alleviates the problem even though the aquifer was generally free of microbial contamination [45]. The main aquifers in SA are impacted by lithogenic and anthropogenic sources.

High aridity and low precipitation are the two main environmental factors responsible for the country's meager surface water resources; this necessitates improved knowledge and mapping of the country's existing freshwater resources. Most aquifer resources in hard rocks are found in fractured and jointed rocks, whereas unfractured rocks contain very little groundwater. 57% of the studied region consists of igneous rocks, whereas 43% consists of sedimentary sequence and Quaternary deposits [46]. The only source of freshwater that replenishes SA's aquifers is precipitation. The precipitation seldom occurred in a relatively brief period and for unexplained reasons. Overexploitation of the hard rock aquifer resulted in a dry well and submersible pump damage. Consequently, aquifer productivity falls, which has a detrimental impact on agricultural goods and the living conditions of inhabitants. Tabuk province, located in the northwest of SA, is one of the promising regions for agricultural expansion and tourism (Figure 1). In this region, groundwater is the only water source for domestic, agricultural, and industrial use. The terrain elevation of the basin is large and steep (reaches 3000 m), implying that most precipitation turns into runoff and flows directly to the ocean. One of the major issues that Tabuk is currently dealing with is the freshwater crisis caused by temperature and rainfall fluctuation. Population growth, agriculture, industry, and tourism require more water consumption, exacerbating the water crisis [47]. About 1,730,767 ha of land were equipped

during the 2000 period for irrigation, meaning an average increase of 0.9%/year since 1992. Only around 70 percent were actually irrigated with groundwater resources [48]. The scientific board is attempting to manage water usage to address this issue. Because of the need for water supply, detecting and managing aquifers is a major concern in Tabuk. The investigated aquifers were coastal and characterized by seawater intrusion (Figure 1). It dramatically changed the groundwater into unsuitable for utilization. The diffusion zone length and wide depend on aquifer geology, hydrogeology, pumping rate, recharge, and anthropogenic sources.

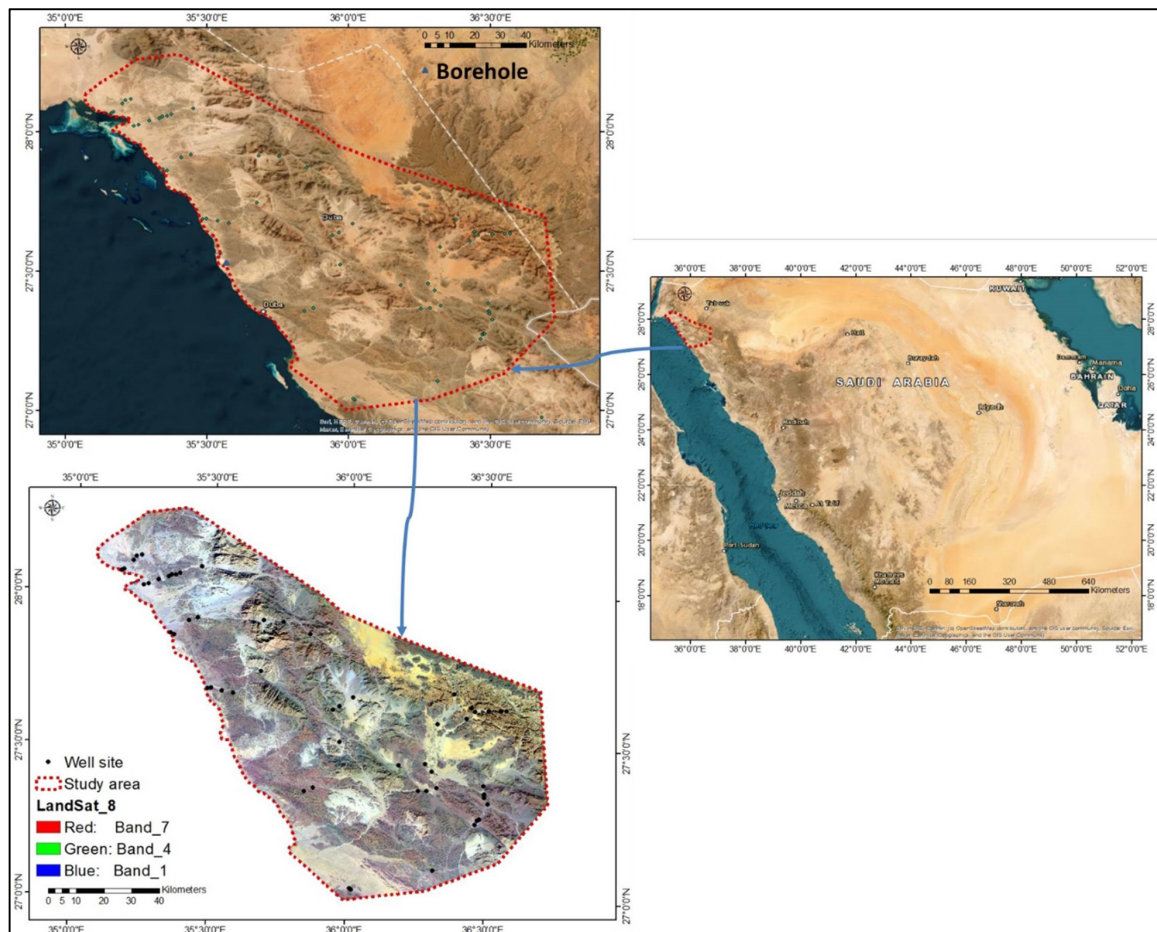


Figure 1. Map of the study area.

The main parameters controlling ARPZ are evaluated based on their impact and influence on water leakage and surface runoff. These factors are soil lithology, land use/cover, lineament density, hydrography expressed as slope, and drainage density [49]. These parameters have the most effective and reliable impact on the aquifer recharge potentiality. In most scientific studies, the criteria for delineation of aquifer recharge potentiality zones have often been used for geomorphology, geology, drainage density, soils, lineament, and land use [50–52]. In the current study, geological, hydrogeological, and hydrological data were used to determine prospective extraction zones for aquifers. The findings identify the most lucrative regions for aquifer exploration and exploitation, which support increased urbanization, agriculture, and investment. People who live in the coastal region rely primarily on groundwater resources, and for them, the water supply is the most alluring problem that worsens the balance of population density between rural, urban, coastal, and desert areas.

The urgency of this study was attributed to the water demand in SA being lower than the water supply. The annual consumption of freshwater resources during 2010 was

$17.9 \times 10^9 \text{ m}^3$ and is predicted to be 19.5×10^9 in 2050 [53,54]. The continual increase in population growth puts pressure on the water supply and needs much more water resources. The population density increased from 27.6 to 32.6 to 38.5 to 45.5 to 53.8 million in 2010, 2015, 2020, 2025, and 2030, respectively [55]. Another reason for the importance of this research was to redistribute population density through SA. The groundwater exploitation and exploration in urban, rural, and desert zones attract dwellers and Bedouins to invest, especially in agriculture, which is beloved to them. Therefore, the population density redistributes itself among all zones of SA not localized in urban areas. The main recharge aquifers were rainfall, which was low values and very rare. They are 100–200 mm/year in the north and <100 in the south, except near the coast, annual rainfall drops below 100 mm. Long-term average annual precipitation has been estimated at $245.5 \text{ km}^3/\text{year}$, which is equal to 114 mm/year over the whole country (AQUASTAT Survey 2008). The aquifer abstraction increased in SA to reach $17 \times 10^6 \times 10^6 \text{ m}^3/\text{year}$ in the last three decades [56]. About 80% of water supply demand was from aquifer water resources [57]. The net annual groundwater recharge is very low with respect to aquifer pumping. The declining groundwater levels also impact its quality [58].

2. Study Area

The investigated area is located in the Duba city of Tabuk province on the Red Sea coast, northwest of SA, between 35° to $36^\circ 30' \text{ E}$ and 27° to $28^\circ 10' \text{ N}$. Duba is known as the “Pearl of the Red Sea” by locals. It is divided into three valleys: Dahkan to the north and Salma and Kafafah to the south [59]. Duba is a port city from which ferries and ships to Egypt and Jordan depart. Egypt’s ports of Hurghada and Safaga can be reached by ferry in about 3 h (minimum) [59]. SA’s most innovative projects and multibillion-dollar investments are in this area. In the futuristic urban development of NEOM, the area is constructing “tomorrow’s world” by fusing natural wonders with cutting-edge technologies. The NEOM, AMAALA, and Red Sea projects will encourage rapid growth and investment throughout the region’s essential sectors as SA’s largest mega project and a key initiative of Vision 2030. By the Red Sea, Tabuk is a growing tourist destination. In addition to offering a mix of desert and coastal landscapes, the area also has some interesting historical sites. In addition to its natural resources, several significant projects, such as AMAALA and the Red Sea Project, are positioning the area as one of the top tourist destinations in SA. The completion of AMAALA, a luxury travel destination with 3000 hotel rooms and wellness, sports, arts, culture, sea, sun, and lifestyle activities, is scheduled for 2027. The Red Sea Project, which includes 90 pristine islands and miles of expansive desert and mountain vistas, is the largest regenerative tourism project in the world (<https://www.investsaudi.sa/en/meetTheKingdom/province/tabuk>; accessed on 23 April 2023).

2.1. SA Water Requirement

The dramatic rise in living standards, population density, and development has resulted in an increased demand for water supply. Sustainable water resources yield in SA was $6440 \times 10^6 \text{ m}^3$ in 2010 and $8720 \times 10^6 \text{ m}^3$ in 2014 (Figure 2). Water demand exceeded yield in 2014 (Figure 2a,b), negatively impacting agriculture and domestic sectors. Because aquifer withdrawal remained constant between 2010 and 2014 (Figure 2a), the current study is concerned with increasing conventional sources (aquifer pumping) to meet the increase in total demand. This research outcome can add a new water supply to coastal villages, increasing agriculture and domestic use. The projected population growth over various time periods necessitates a significant increase in water supply (Figure 2c,d), which has been partially addressed by adding new promising areas, as demonstrated by current research. In 1960, the population density was 4 million, which will rise to 59.5 million by 2050 (Figure 2c,d) [53,54].

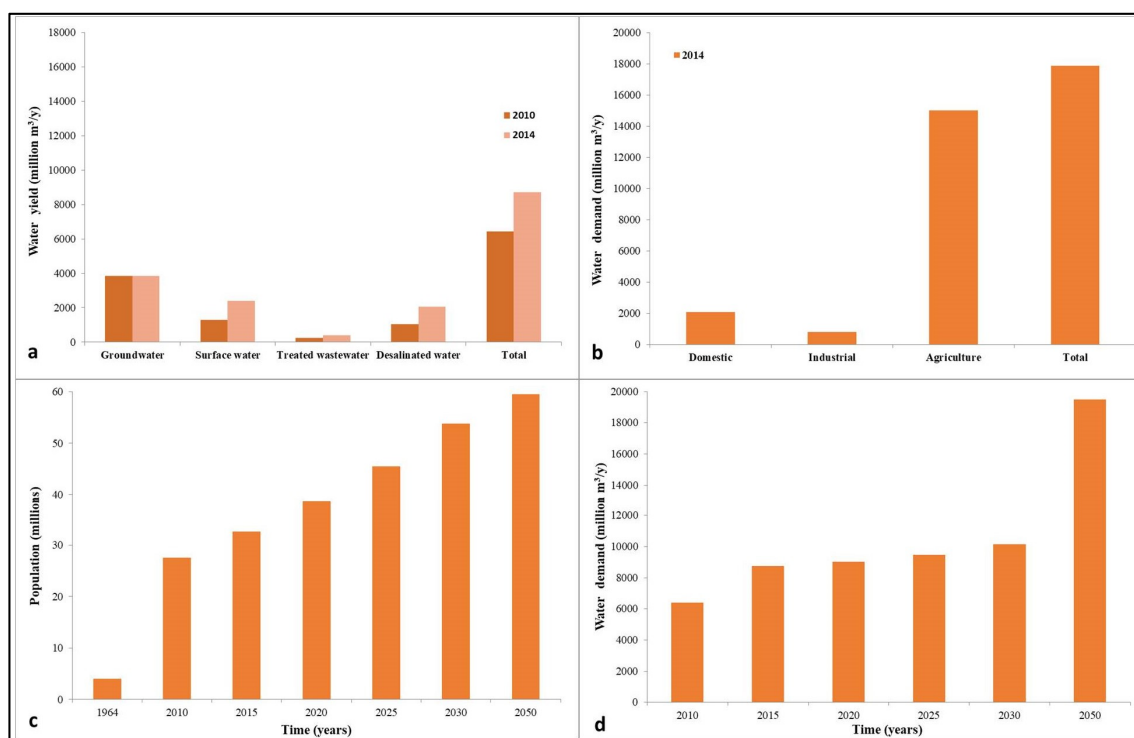


Figure 2. (a) Sustainable water resources yields (b) water demand in different sectors, (c) estimated population, and (d) estimated water demands in SA [55,60].

2.2. Geology

The first western coastal geology was known as the Arabian Shield (hard rocks), and the second eastern section was known as the sedimentary section [61]. The study area contains rock units from various periods (Figure 3). Figure 4a depicts the sedimentary formation and igneous units. Sandstones, conglomerates, siltstones, and thin carbonate layers make up the Oligo–Miocene sedimentary deposits. The wadi alluvial primarily represents Quaternary sediments [62].

In Figure 5, the sedimentary cover and alluvium deposits were extracted, indicating excellent aquifer porosity and permeability, accounting for approximately 43% of the geology.

The highest geology surface area (>100 km²) was depicted in Figure 6, while the remaining geology area was less than 100 km². Quaternary sand, gravel, and silt deposits had the most surface area, followed by Ram and Umm Sahm sandstones, Ghawjah formation, andesitic lavas, porphyritic amphibolite, and pyroclastic rocks, Haql suite, Shatisyenogranite to al-kali-feldspar granite (Figure 5). Previous geology, which was characterized by high porosity, permeability, and leakage, was the primary source of aquifer potential. Figure 4b depicts the subsurface geology of the borehole beside Duba (the coastal zone between Hasha and Almazaraa). The maximum depth of the well was 20 m. From top to bottom, the lithological units were man-made fill, compacted soft and fractured sandstone, and light brown to grey, hard, and massive sandstone (Figure 4b).

2.3. Hydrogeology

Because precipitation in SA was minimal and unknown, it is classified as an arid region. The high streams (1st to 7th orders) carry surface water and recharge the aquifer system (See Figure 11a). The aquifer was a critical water resource in SA, particularly in coastal villages. The sedimentary cover and alluvium deposits in the study area represent the aquifers (Figure 5). The Saq aquifer is one of the largest (6500 km²) in the study area and contains 280,000 mm³ of water [63,64]. It is referred to as a transboundary aquifer because it stretches from Jordan to the northern part of Saudi Arabia. The aquifer was

restricted because it was capped by clay, grey shale, and siltstone (Figure 4b). The effective porosity ranged between 0.10 and 0.20 [65], and the aquifer age ranged between 22,000 and 28,000 years ago [66]. The transmissivity ranged between 1400 and 1728 m²/d, while the storativity ranged between 0.00015 and 0.000362 [63].

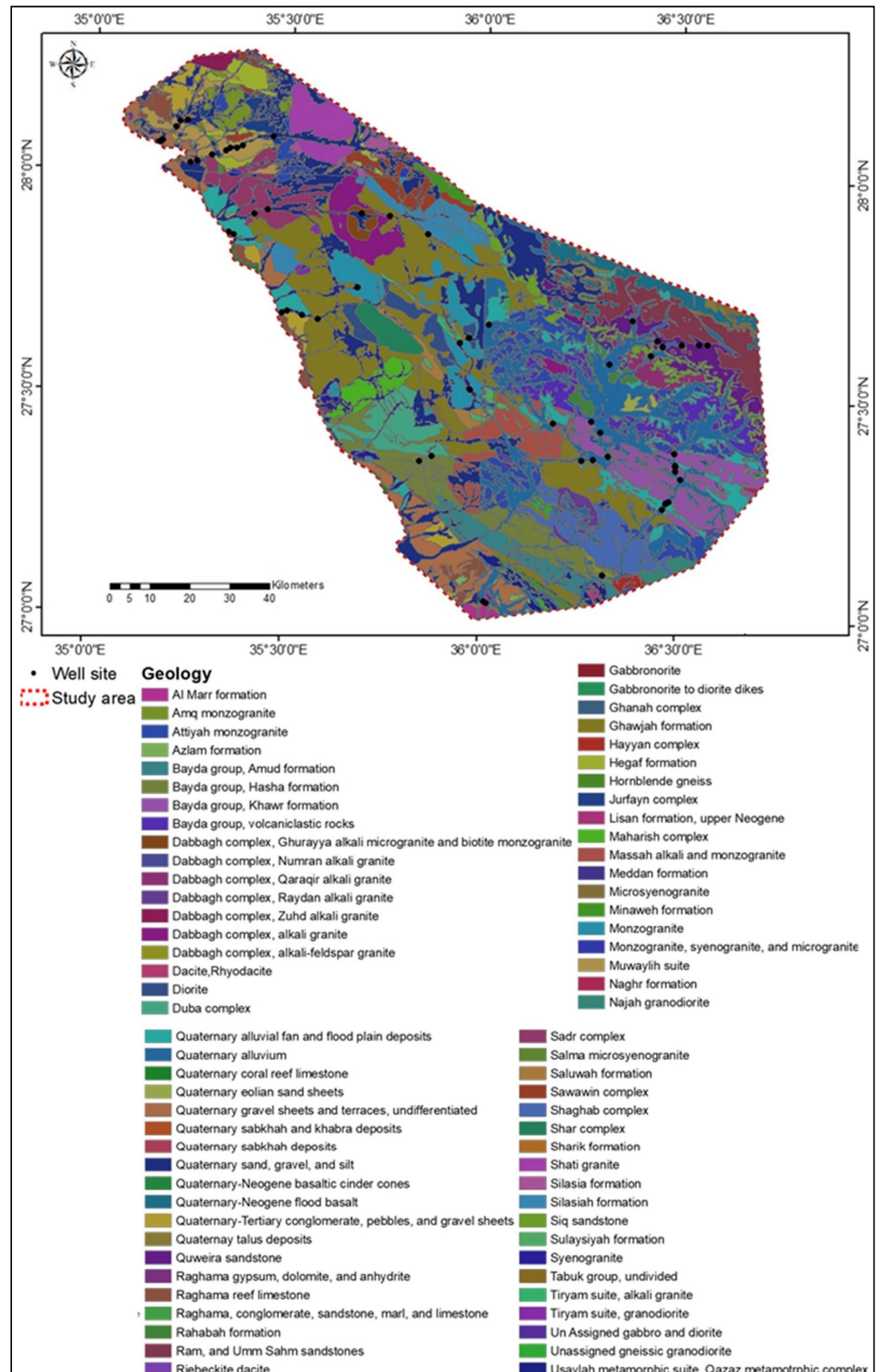


Figure 3. Geology of the study area.

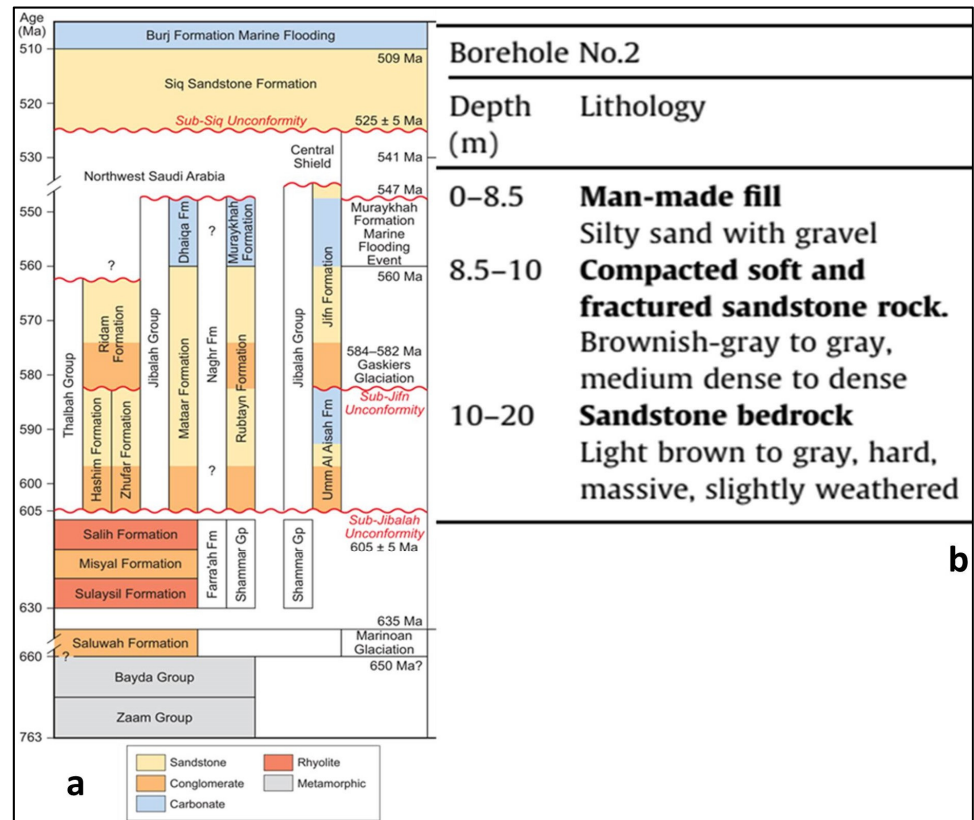


Figure 4. (a) Composite stratigraphic column and (b) subsurface borehole in northwest SA (after [62]).

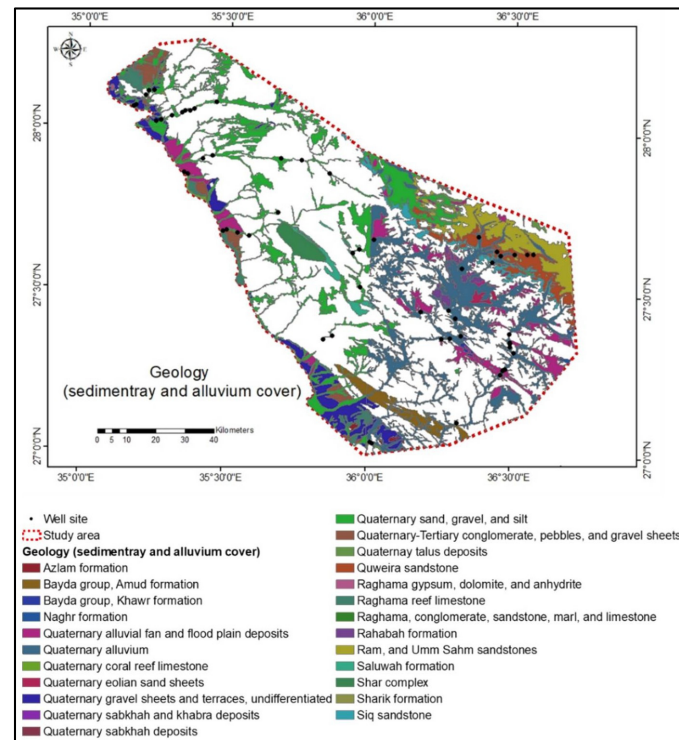


Figure 5. Geology of sedimentary cover and Quaternary deposits.

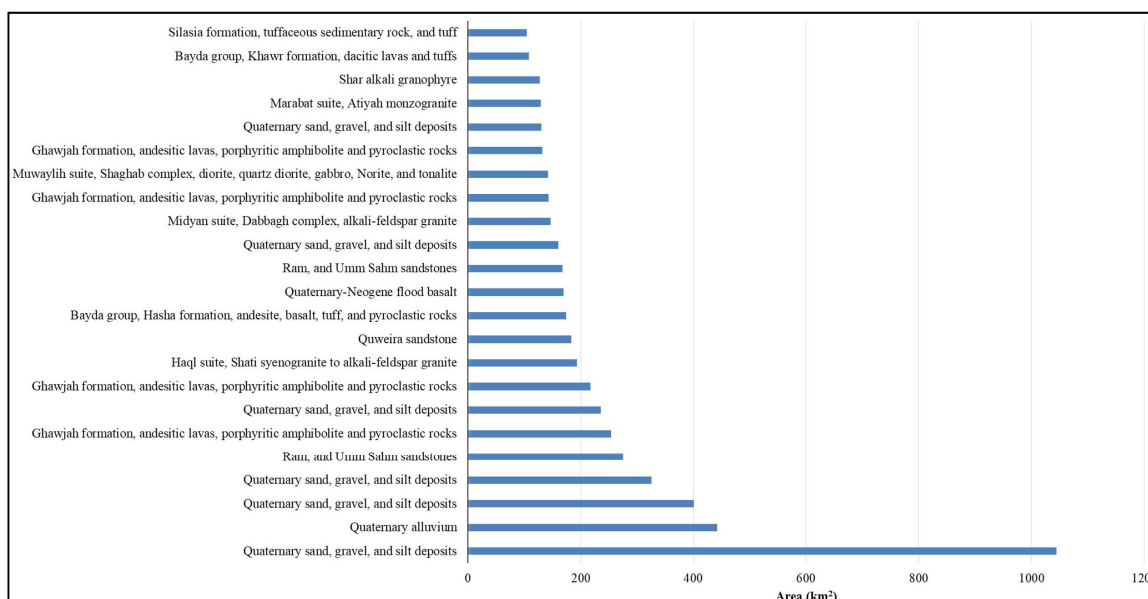


Figure 6. Areal distribution of the geology in the study area of greater than 100 km².

3. Methodology

3.1. Data Used

Three 30 m spatial resolution Shuttle Radar Topographic Mission (SRTM) DEM images were downloaded from the website (<https://earthexplorer.usgs.gov/>) and merged using ArcGIS 10.3 software. The drainage watersheds were outlined using ArcGIS 10.3 software tool (Hydrology option). Four LandSat 8 (L8) satellite images with “UTM WGS84” ZONE 36–37 were acquired: LC81720412021353LGN00, LC81720422021353LGN00, LC81730402021360LGN00, and LC81730412021360LGN00. They were mosaicked and pre-processed using ENVI 5.1 software. Flowchart of the methodology applied for ARPZ is shown in Figure 7.

3.2. Procedures

For overlay and analysis, eight thematic parameters were prepared: surface geology, rainfall, lineaments density, drainage density, slope, elevation, soil, and NDVI. The SRTM-DEM extracted patterns of elevation, slope, and drainage. The lithological exposure (shapefiles) was downloaded from the SA webpage (<https://ngp.sgs.gov.sa/>; accessed on 23 February 2023). NDVI and lineaments were derived from satellite images. The rainfall (2021) and soil data were gathered from the website (<https://data.chc.ucsb.edu/products/CHIRPS-2.0/global/annual/tifs/>; accessed on 2 March 2023).

3.3. Automatic Lineaments Extraction

The L8-OLI comprises eleven bands of low cloud cover (0.02). Lineaments are linear or curved edges connected with geologic formations (joints, fractures, line weakness, and fault planes). Human activities were removed from the map of lineaments. From satellite images, lineaments (geologic features and tectonic fabrics) were recovered (multispectral L8). This research employs the first principal component image (PC1) of L8 pan-sharpened reflected bands. PC1 is suitable for lineament extraction as it contains most of the information. ENVI 5.1 transferred the PC1 (8-bit grayscale) image (15 m spatial resolution) to PCI Geomatica software version 2016.0 for automatic lineament delineation. ArcGIS 10.3 was used to coordinate the lineaments and construct lineament density. Latitudes and longitudes of the lineament (X1, Y1, X2, Y2) are exported from ArcGIS 10.3 to the Rockworks version 17 software to create the rose diagram. The NDVI was calculated employing ENVI version 5.1.

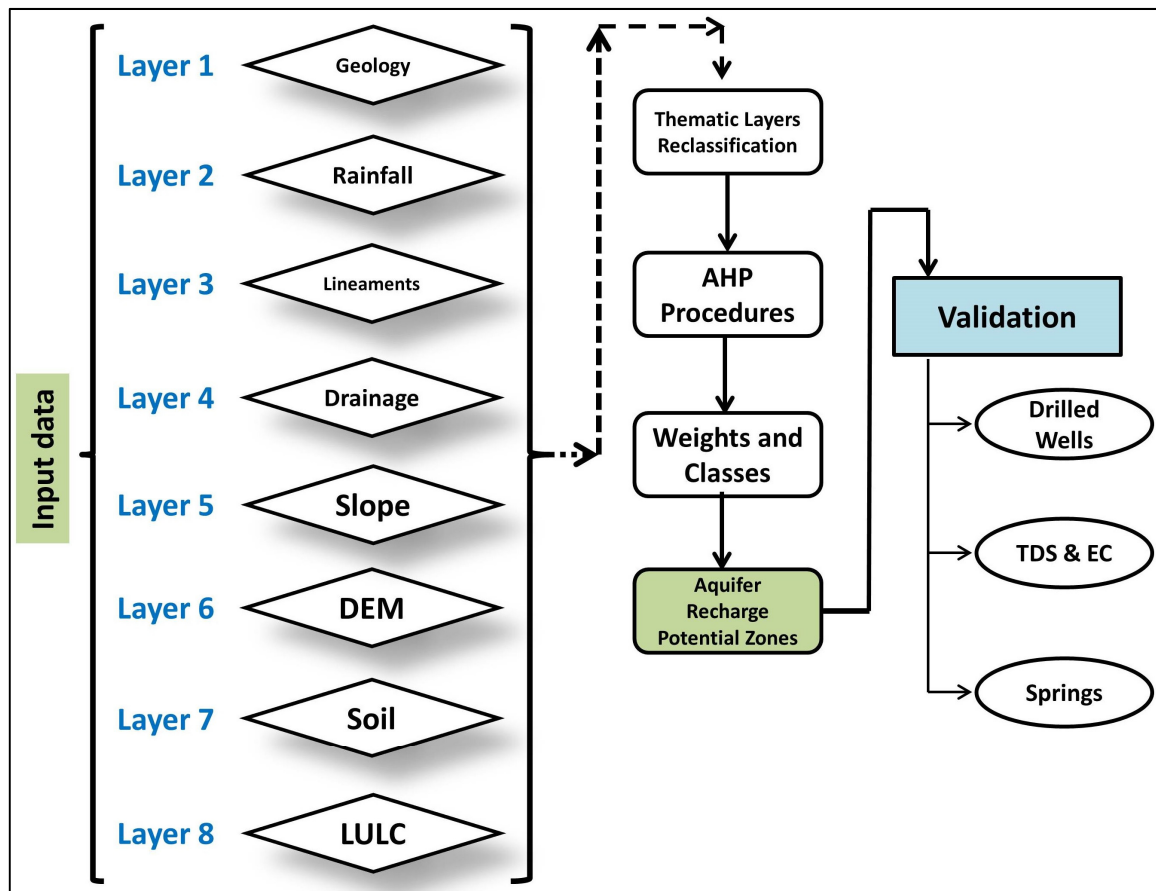


Figure 7. Flowchart of the methodology applied.

3.4. Aquifer Potentiality Map and Verification

The eight thematic layers were stratified by GIS based on the contribution weights for aquifer recharge potentiality (Tables 1 and 2). By combining all the spatial layers with weighted overlay trends, the potential areas for aquifer recharge were determined. Before the overlying operation, individual spatial layers were reclassified by GIS techniques to a uniform rank of 1–5, except soil which is 1–4, with 1 denoting the lowest aquifer potential and 5 denoting high aquifer recharge potentiality. Based on AHP, weights were inputted into a pairwise comparisons matrix (Table 1). Based on field survey experiences and existing literature [24,67,68], the ranks were chosen for the corresponding inputted criteria. Surface geology (lithology) was assigned the highest weight, whereas NDVI was assigned a low weight, and the rest parameters were in-between the two (Table 2). Rainfall, the only recharge for aquifer potentiality, is the second-highest weight parameter, followed by lineaments, which account for the permeability of groundwater flow (Table 2). The drainage density, topography, and soil characteristics come after them (Table 2). The NDVI was given the lowest weight because it has the smallest agricultural regions and low NDVI values due to high temperatures and evaporation. There were various hard rocks, sedimentary deposits, and alluvial sediments in the surface geology (lithology). Hard rock lineament patterns ranged from hydrogeologically connected (high permeability) to unconnected (separate) with poor permeability. Individual sub-variable ranks were provided once the corresponding parameters were assigned weights [69–71]. The weights in Table 2 were estimated as in Table 1 and Table S1 and used to determine the influence impact, equal to weight multiplied by 100. The maximum value describes the highest groundwater potentiality and vice versa. According to its capacity to contribute to aquifer recharge, each parameter's ranking in Table 2 was determined. The calculation method in Table 1 is shown in Table S1. The ARPZ extraction was processed based on the flowchart

(Figure 7). The aquifer recharge potentiality resulted from the overlay and ranged from very low to very high ARPZ. The high to very high aquifer recharge potentiality matches with drilled wells and hydrogeochemical parameters concentration of the aquifer (TDS, EC, Br, Sr, and NO₃).

Table 1. Normalized Pairwise comparison matrix (eight layers) developed for AHP-based groundwater potential zoning.

Parameters	Lithology	Rainfall	Lineaments	Drainage	Slope	Elevation	Soil	NDVI	Weight
Lithology	8	7	6	5	4	3	2	1	0.37
Rainfall	8/2	7/2	6/2	5/2	4/2	3/2	2/2	1/2	0.18
Lineaments	8/3	7/3	6/3	5/3	4/3	3/3	2/3	1/3	0.12
Drainage	8/4	7/4	6/4	5/4	4/4	3/4	2/4	1/4	0.09
Slope	8/5	7/5	6/5	5/5	4/5	3/5	2/5	1/5	0.07
Elevation	8/6	7/6	6/6	5/6	4/6	3/6	2/6	1/6	0.06
Soil	8/7	7/7	6/7	5/7	4/7	3/7	2/7	1/7	0.05
NDVI	8/8	7/8	6/8	5/8	4/8	3/8	2/8	1/8	0.046

Table 2. Weights assigned for different aquifer control parameters in DubaCity (after Roy et al. [72]).

Parameter	Classes	Weight	Influence (%) = Weight × 100	Rank
Lithology	Quaternary deposits	0.37	37	5
	Sedimentary succession			5
	Fractured and jointed hard rocks			4
	Less fractured and jointed hard rocks			2–3
	Nonfractured and jointed hard rocks			1
Rainfall (mm/year)	18.25–27.65	0.18	18	1
	27.66–37.05			2
	37.06–46.45			3
	46.46–55.86			4
	55.86–65.25			5
Lineaments (km/km²)	0–0.22	0.12	12	1
	0.23–0.44			2
	0.45–0.65			3
	0.66–0.87			4
	0.88–1.09			5
Drainage (km/km²)	0.15–0.82	0.09	9	1
	0.83–1.08			2
	1.09–1.25			3
	1.26–1.44			4
	1.45–2.05			5
Slope (Degrees)	0–6.1	0.07	7	5
	6.11–14.04			4
	14.05–23.19			3
	23.2–34.17			2
	34.18–77.81			1
Elevation (m)	–20–280	0.06	6	5
	280.01–550			4
	550.01–877			3
	877.01–1221			2
	1221.01–2291			1

Table 2. Cont.

Parameter	Classes	Weight	Influence (%) = Weight × 100	Rank
Soil	I-Y-bc	0.05	5	4
	I-YK-2ab			3
	Rc30-1ab			2
	Zo20-1/2a			1
NDVI	−0.118–0.008	0.046	4.6	5
	0.009–0.036			4
	0.037–0.064			3
	0.065–0.101			2
	0.102–0.218			1

4. Results and Discussion

4.1. Thematic Parameters

4.1.1. Surface Geology

The porosity and permeability of the detected aquifers, as well as the recharge rate, are represented by the exposed geology. It affects the characteristics of the soil [73]. Geology is the most influential factor in aquifer recharge because the research area is situated in an arid region characterized by drought due to the lack of freshwater aquifers. The Arabian Shield (igneous and metamorphic rocks), carbonate layers, sedimentary sequence, joints and fractures, and alluvium deposits are among the geologic structures of the study area. They have a significant impact on aquifer development. The investigated area is highly covered by sedimentary and quaternary deposits (Figure 5). Geology (exposed lithology) is directly connected to rainfall recharge, particularly during storm events. Regional expansion and lithology types (porosity and permeability) influence aquifer recharge and potentiality. Based on the porosity and permeability of exposed aquifers, lithology controls aquifer recharge, surface runoff, and flooding. Regarding lithology, one must comprehend the characteristics of rocks in terms of their compactness, weathering status, joints, and fractures. Complex groundwater flow in rocks with limited porosity and permeability indicates the lowest aquifer recharge potential. In contrast, increased aquifer permeability enhanced groundwater flow, confirming the highest aquifer recharge potential.

ARPZ were significantly influenced by extensively fractured and jointed hard rocks (both igneous and carbonate), sedimentary strata, and Quaternary alluvium deposits. The potentiality contribution of shale is represented by class 5 (very high aquifer recharge potential) (Figure 3a–b), whereas non-fractured and jointed hard rocks contributed to class 1 (very low aquifer recharge potential). The potential contribution from geology: class 2 to class 4 (low to high aquifer recharge potential) is based on rock type, porosity, permeability, and hydrogeological correlation of fractures and joints.

4.1.2. Rainfall

After geology, it is the most crucial factor in determining ARPZ, particularly for the current study (arid) region. Precipitation values, duration, and intensity impact the hydrogeology of the aquifer potentiality [74]. Aquifer recharge from precipitation is influenced by exposed geology and infiltration capability [73].

The short duration of intense rainfall that causes low leakage increase runoff, but the long duration of low rainfall encourages aquifer recharge rather than surface runoff. ARPZ is influenced by the region's topography and the yearly rainfall [74–76]. During 2021, rainfall varied from 18 mm/year in the west to 85 mm/year in the east (Figure 8a). The area with the highest rainfall shows a very high aquifer recharge potentiality (class 5). In contrast, the area with the very low aquifer recharge potentiality (class 1) had the lowest rainfall. The contribution to ARPZ (class 1 to 5) based on the rainfall amount is shown in Figure 8b.

About 67% of the studied area shows low and very low aquifer recharge potentiality. The remaining 33% represents moderate to very high aquifer recharge potentiality (Figure 8c).

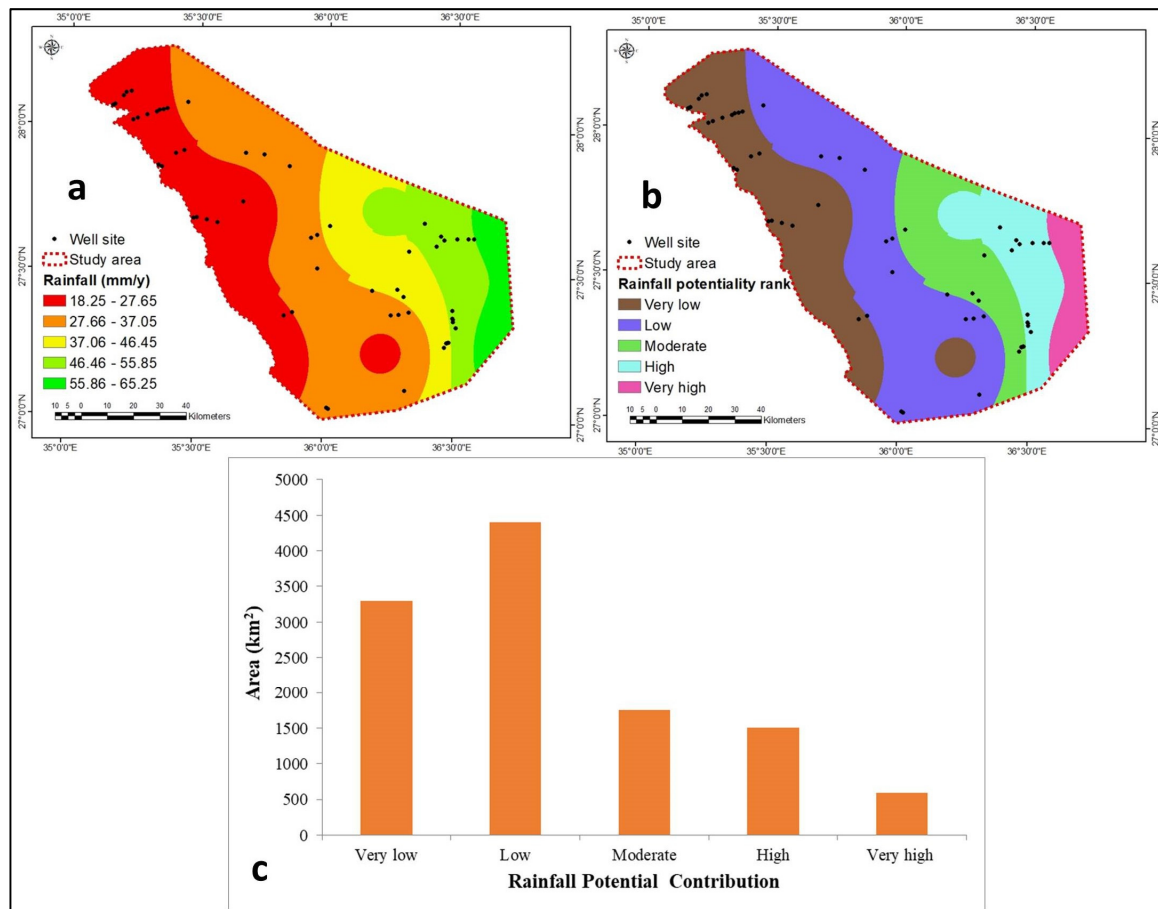


Figure 8. (a) Rainfall pattern, (b) rainfall potential contribution, and (c) areal distribution of rainfall zones.

4.1.3. Lineaments Density

Lineaments are represented by fractures, joints, and fault planes and might be lines or curves [77]. The lineaments represented the hard rock's secondary porosity and permeability (carbonate and igneous). Because of their high porosity and permeability, they significantly impact the aquifer's recharge potentiality [78–82]. Lineaments were used to represent geological structures. The aquifer potentiality was shallower rather than deeper; they were more concerned with lineaments dispersion and hydrogeological interconnection than aquifer potentiality. High aquifer recharge coincides with high lineament patterns and interconnectedness, and vice versa. Underground fractures are indicated by lines resulting from tectonic activity. It is a long, linear geological structure (fault or joint) visible on satellite pictures [19]. Lineaments and faults with moderate to high permeability allow water to leak, increase hydraulic conductivity and secondary porosity, and improve vertical water flow that recharges groundwater [25,83,84].

The distribution, lengths, hydrogeologic connectivity, and depth of the fractures significantly influence ARPZ. There are 3585 lineaments, ranging from 9 to 4495 m in length, with a mean length of 707 m (Figure 9a). The fractures' total length is 2534 km. The NE-SW and E-W fracture trends were predominant (Figure 10). The very high aquifer recharge potentiality (class 5) (Figure 9c) is shown by the zones with the highest lineament concentration (0.88–1.09 km/km², Figure 9b) due to its high secondary permeability.

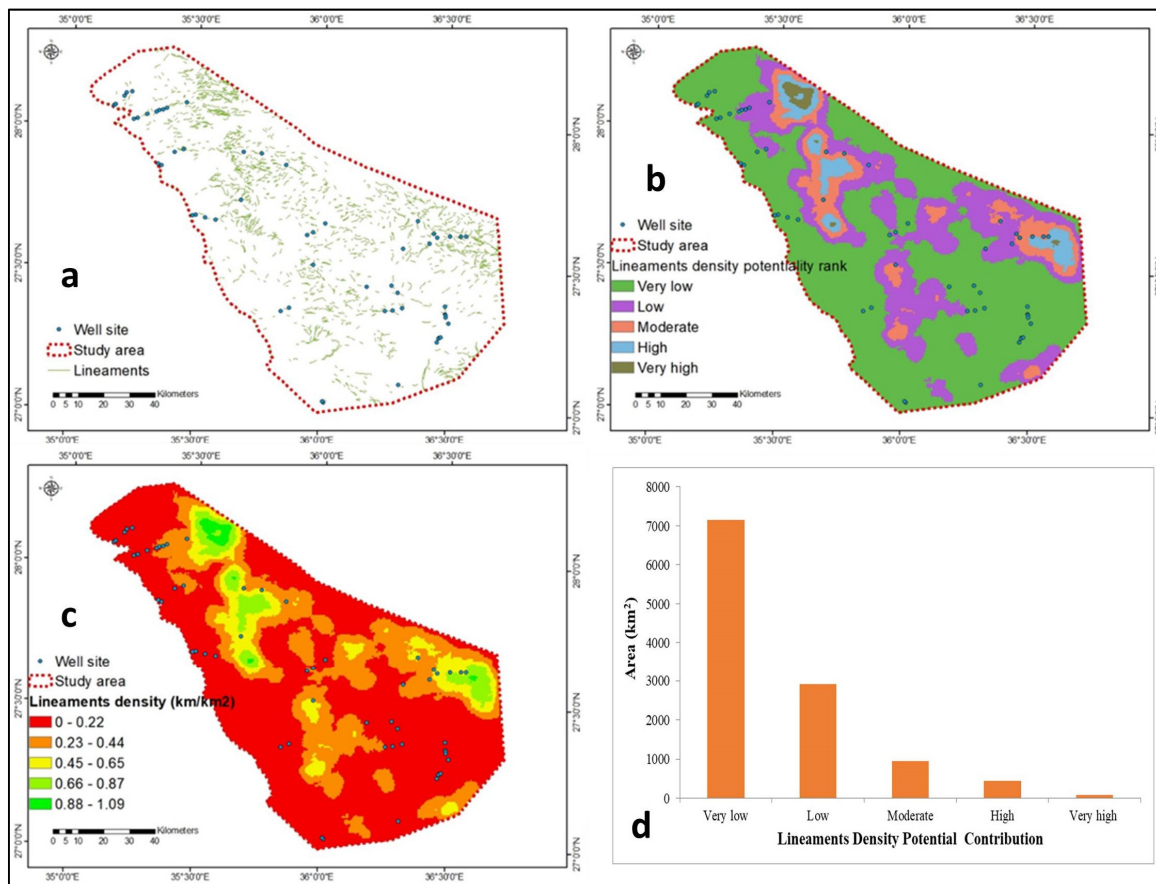


Figure 9. (a) Lineaments, (b) lineaments density, (c) lineaments density potentiality, and (d) areal distribution.

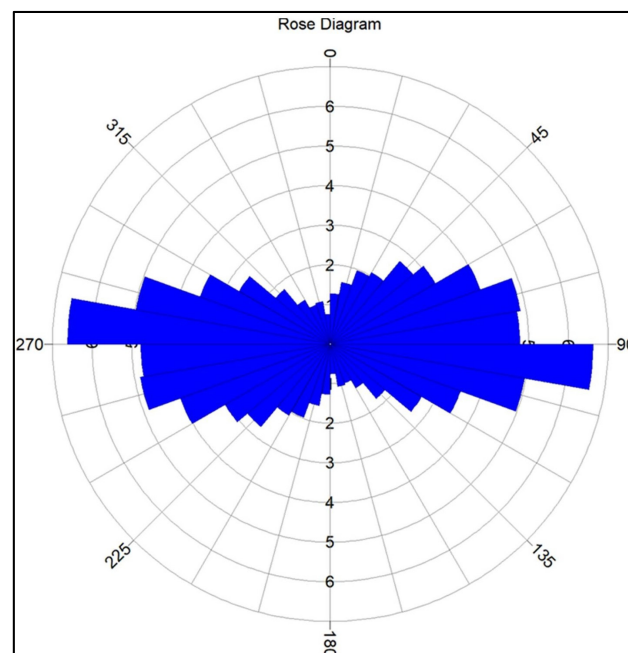


Figure 10. Rose diagram of the fractures system.

The areas with the lowest lineaments density (0–0.22 km/km², Figure 9b) were included in the very low aquifer recharge potentiality (class 1) (Figure 9c). The five classes (1 to 5) of lineaments’ contribution to aquifer recharge potentiality were determined based

on density distribution (Figure 9c). 95% of the study region shows low to very low lineament density, while the remaining 5% exhibits moderate to very high lineament aquifer potential (Figure 9d).

4.1.4. Drainage Density

It measures the distance between stream channels by dividing the sum of stream lengths by the watershed size [85,86]. It depends on the soil's composition, weathering processes, leakage rate, and surface runoff [73,74]. Most of the researchers [49,73–75,85,86] represent the highest drainage density with low rank because they indicate low permeability and low recharge and vice versa. According to the geological investigation, 43% of the exposed rock is sedimentary cover and Quaternary deposits (Figure 5). The remaining is distributed among hard rocks with low to moderate to high fractures and joints. In light of this, the maximum drainage density encourages leakage into the aquifer leakage due to high porosity and permeability and increases aquifer recharge potential. Therefore, high drainage density indicated a very high aquifer recharge potential (class 5), whereas low drainage density represented a very low aquifer recharge potential (class 1). The study area was distinguished by 7th order (Figure 11a) and subdivided into five classes based on drainage density distribution ($0.15\text{--}2.05\text{ km/km}^2$) (Figure 11b). The lowest drainage density ($0.15\text{--}0.82\text{ km/km}^2$) contributed to class 1 (Figure 10c), whereas the highest drainage density ($1.45\text{--}2.05\text{ km/km}^2$) contributed to class 5 (Figure 11c). Figure 11c shows the aquifer recharge potential between class 2 to class 4 based on drainage density values. The very low to low drainage density ARPZ represents about 9% of the study area, while the rest 91% exhibit moderate to very high drainage density aquifer recharge potential (Figure 11d).

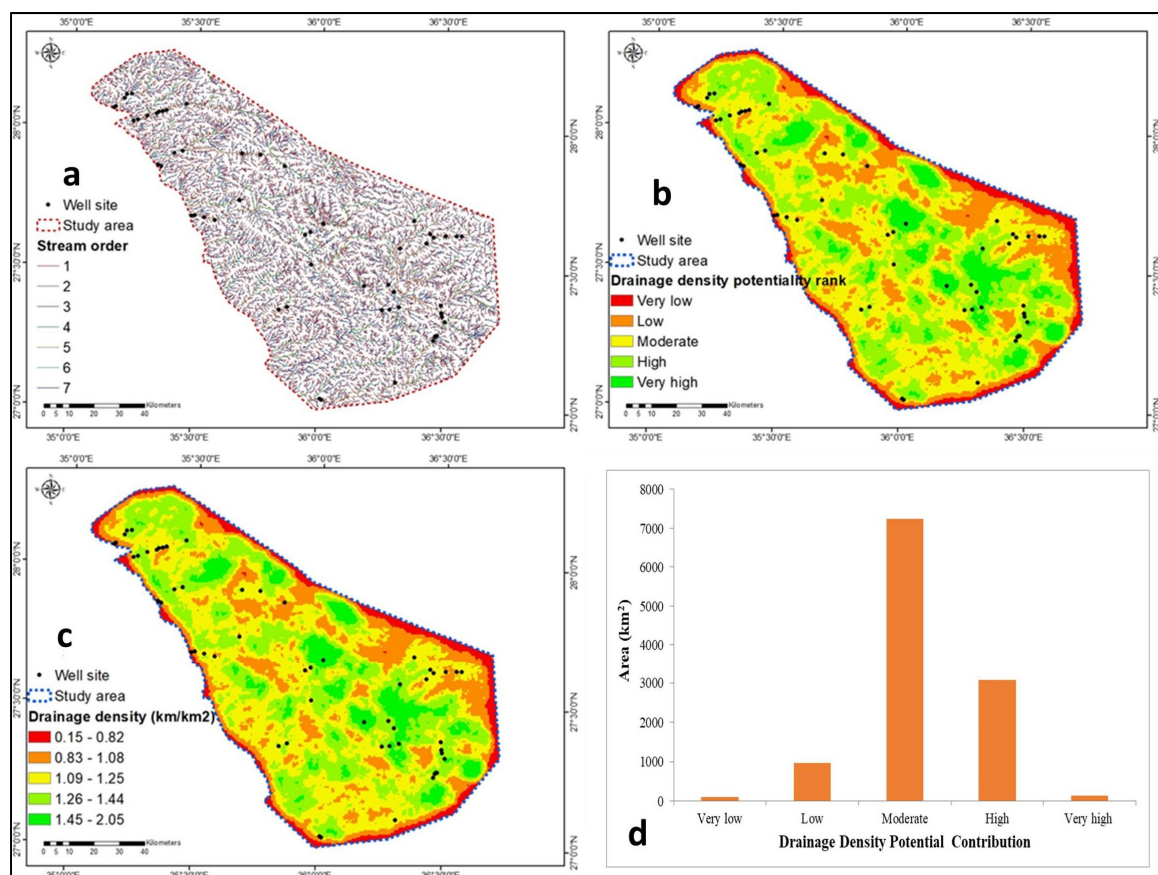


Figure 11. (a) Stream order, (b) stream density, (c) stream density potentiality, and (d) area distribution.

4.1.5. Slope

The drainage basin's boundary shape impacted how much surface runoff flowed off, was retained, and recharged into the aquifer. They are significantly affected by slope and topography. High surface runoff, low water seeping into the aquifer, and low aquifer recharge potential were characteristics of the steep slope regions. On the other hand, gentle slopes were distinguished by low surface runoff, high infiltration, and high aquifer recharge potential. The study area's slope varied from gentle (0 degrees), which was centered in the southwest, to 77.81 degrees, which was centered in the southeast and central region (Figure 12a). The slope map divided into five classes (1 to 5) starts from very low to very high aquifer recharge potentiality and corresponds to slopes ranging from 34–78 degrees and 0–6.1 degrees, respectively (Figure 12a,b). The very low to low ARPZ represents 14% of the study area, while the moderate to very high aquifer recharge represents the rest, 86% (Figure 12c).

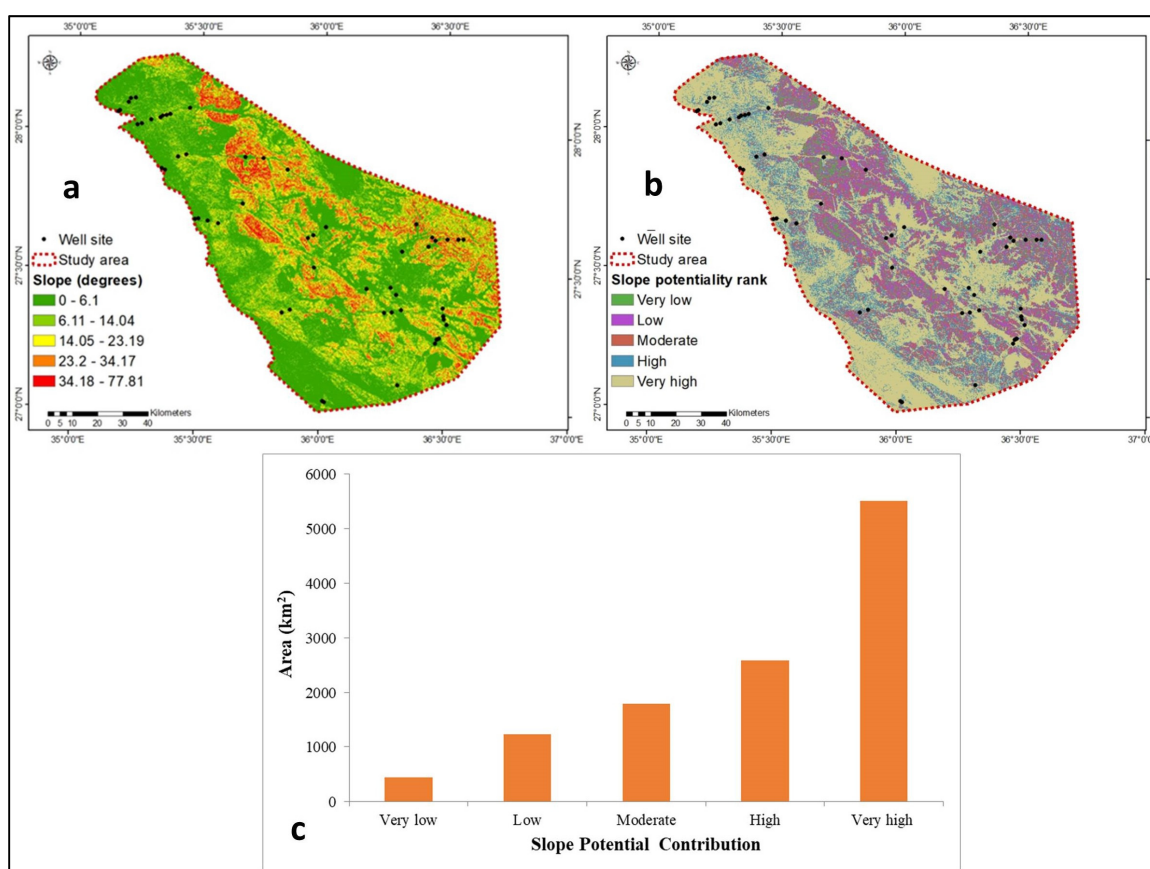


Figure 12. (a) Slope, (b) slope potentiality, and (c) areal distribution.

4.1.6. Elevation

The topography positively correlates with surface runoff and inversely with leakage into an aquifer and recharge rate. Higher topography has the lowest aquifer recharge potentiality (class 1) because it has low infiltration rates and high surface runoff. The highest aquifer recharge potentiality (class 5) is represented by low topography because it increases infiltration and enhances aquifer recharge [74,87]. Based on the elevation range (−20 to 2291 m above sea level), the study area was divided into five classes (1 to 5), with the very high (class 5; 1221–2291 m) and very low (class 1; −20–280 m) aquifer recharge potentiality corresponding to the highest and lowest elevation ranges, respectively (Figure 13a,b). About 18% of the research area represents very low to low aquifer recharge potentiality, while the remaining 82% shows moderate to very high ARPZ (Figure 13c).

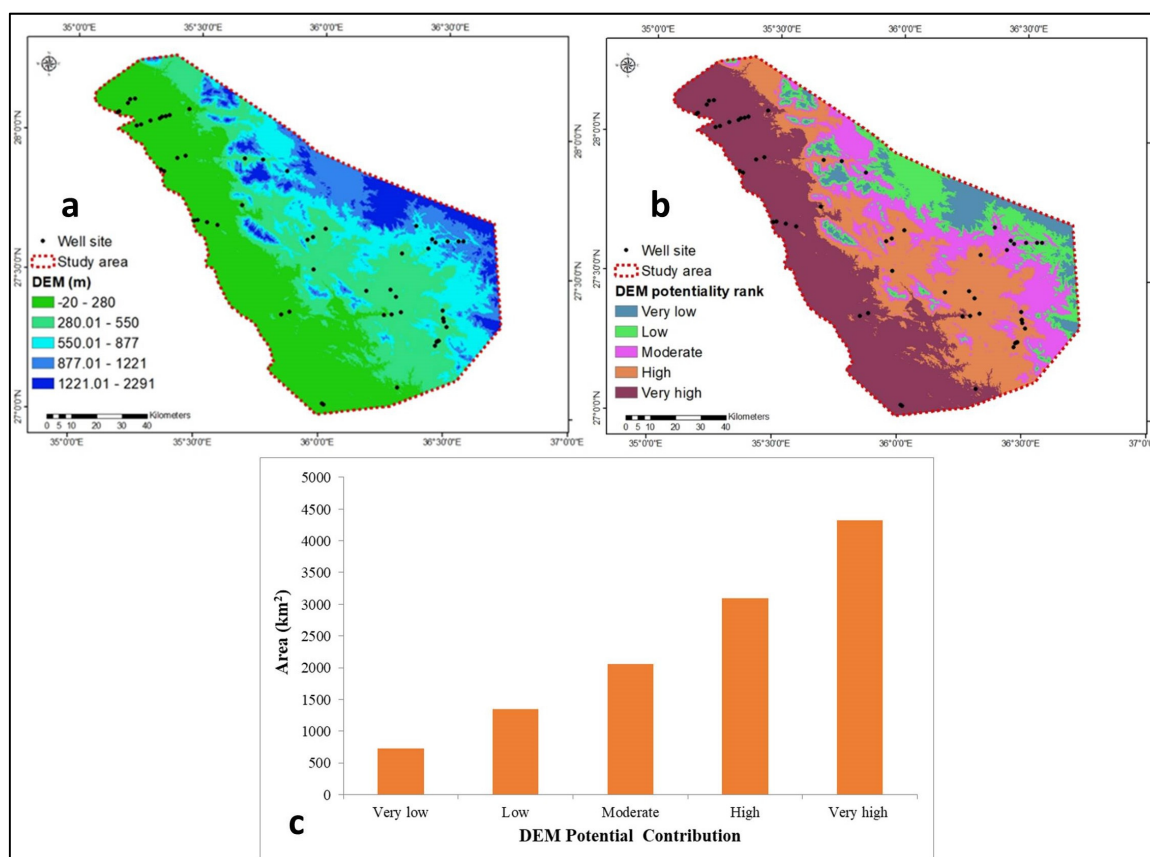


Figure 13. (a) Elevation, (b) elevation potentiality, and (c) areal distribution.

4.1.7. Soil

The soil's porosity and permeability influence the hydrogeologic interconnection between surface and groundwater. Leakage and aquifer recharge are impacted by the properties of the soil's structure and texture [28,74,85]. The coarser soil lithology increases the aquifer recharge potentiality and vice versa [88]. The soil types with the most gravel and sand content have high aquifer recharge potentiality (class 4), which promotes infiltration and recharge.

The very low aquifer recharge potentiality (class 1) is due to the finest soil textures (clay and silt), which increase surface runoff and decrease infiltration rates [28]. The soil characteristics were divided into four categories, namely, I-Y-bc, I-YK-2ab, RC30-1ab, and Z020-1/2a, corresponding to very high, high, medium, and low aquifer recharge potentiality (Figure 14a). About 85% of the study area's soil represents high and very high aquifer recharge potential. In contrast, the other 15% shows medium and low potential (Figure 14b).

4.1.8. NDVI

The NDVI (vegetation cover) is represented by using RS data. The NDVI ranged between 1 and -1 . In accordance with Table 3, the NDVI range of 0.4–1 is attributed to good aquifer recharge potentiality and recharge; however, when it declines, the aquifer recharge potentiality decreases because of low vegetation cover.

The NDVI has been divided into five categories based on aquifer recharge potentiality, namely, extremely low (-0.118 – 0.008), low (0.009 – 0.036), moderate (0.037 – 0.064), high (0.065 – 0.101), and very high (0.102 – 0.218) (Figure 15a,b). About 39% of the region under investigation fell into the low and very low category, while the remaining area (61%) represents moderate to very high aquifer recharge potential (Figure 15c).

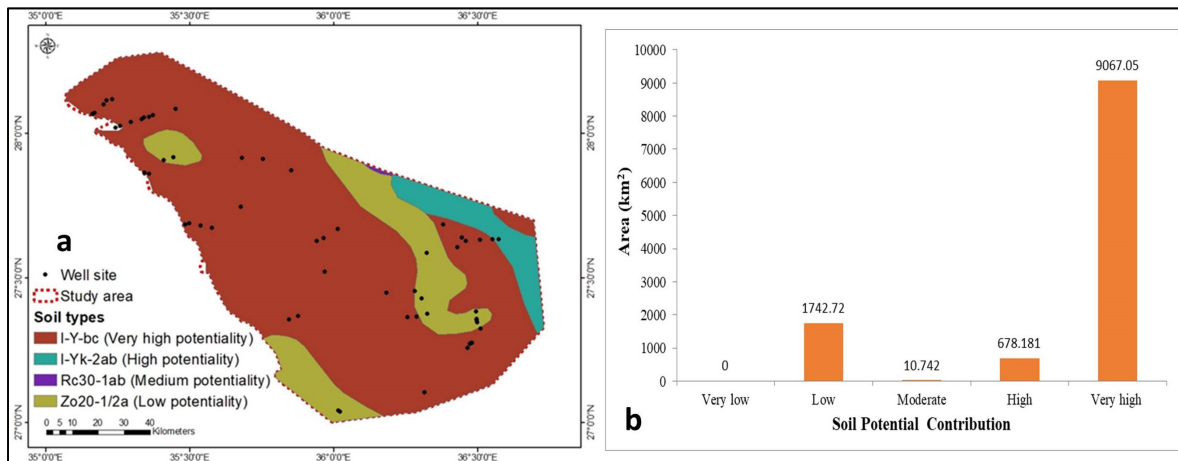


Figure 14. (a) Soil types and (b) areal distribution.

Table 3. NDVI classification features.

NDVI	Features
$\leq -1-0$	Snow, water, sand, and cloud
0–0.1	Bear rock, barren land, or built-up area
0.1–0.2	Shrub and grassland
0.2–0.4	Sparse vegetation or senescing crops
0.4–0.8	Vegetation
0.8–1	Very healthy dense vegetation

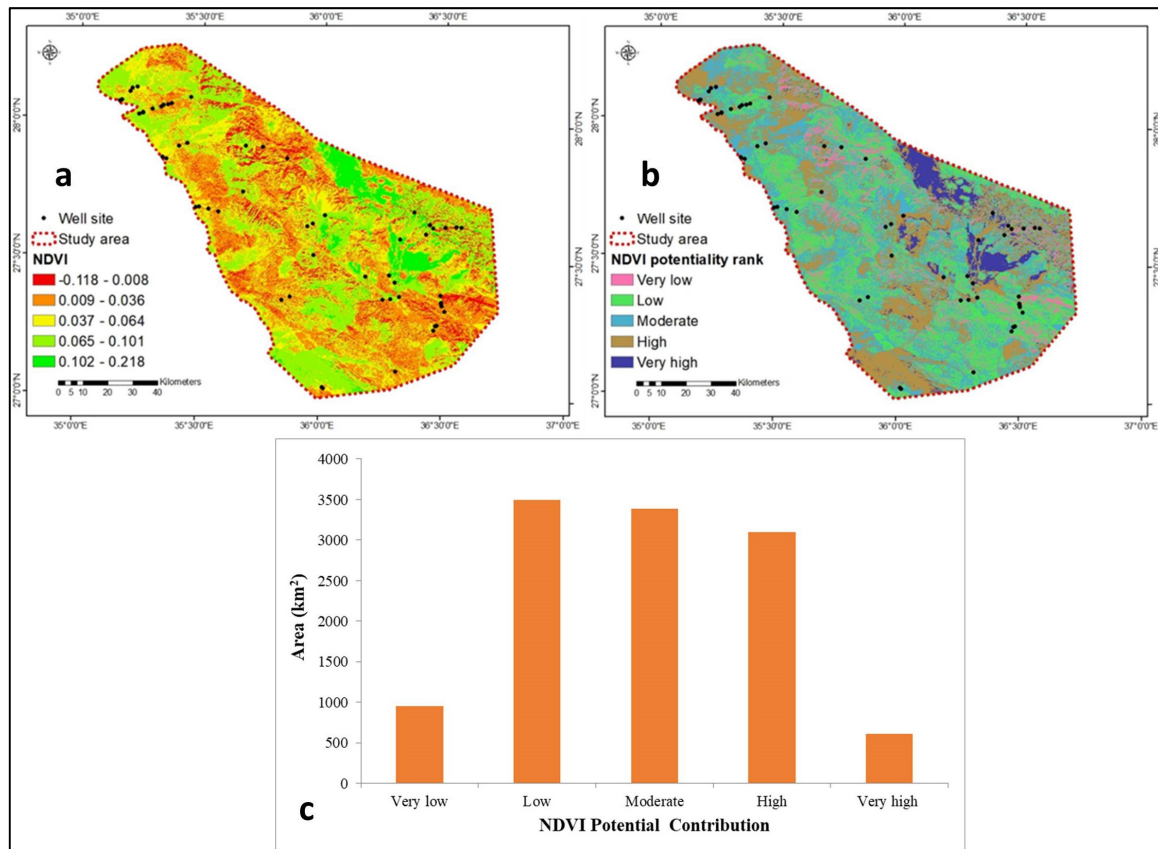


Figure 15. (a) NDVI values, (b) NDVI potentiality, and (c) areal distribution.

4.2. Aquifer Potential Recharge Zones (ARPZs)

The map of ARPZ is significant in agricultural, domestic, and industrial management and was derived from several geological, hydrogeological, and hydrological thematic maps. Each parameter's weight is determined by how much it contributes to groundwater recharge (Table 2). The most promising map of the ARPZ integrated by these thematic maps was predicted using RS, GIS, and AHP techniques. In the current research, the groundwater potentiality recharge was influenced by surface geology, rainfall, lineament density, drainage density, slope, elevation, soil, and NDVI parameters. These eight maps comprising the above parameters were superimposed to produce a single map that identifies the most crucial ARPZs (Figure 16).

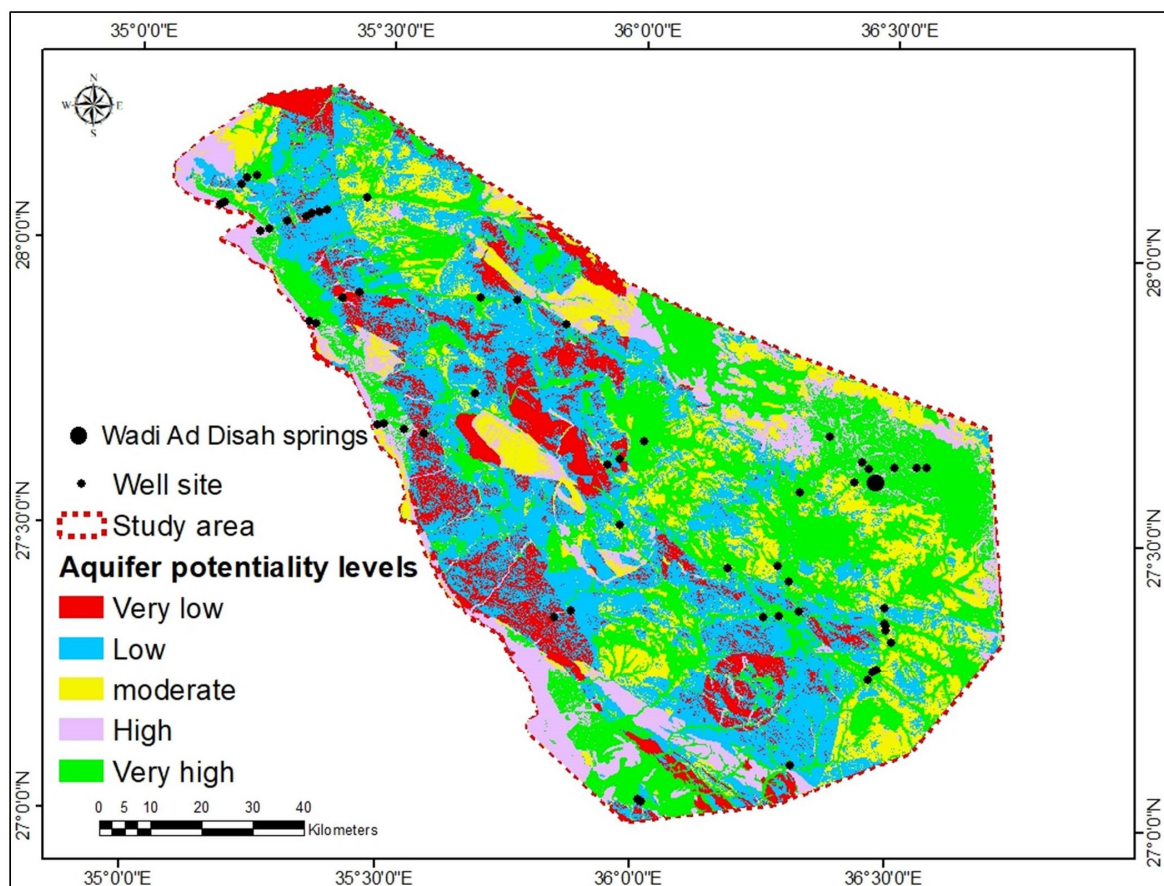


Figure 16. Aquifer potential recharge zones (ARPZ) map of the study area.

GIS-weighted thematic layers have been used to extract the aquifer potentiality distribution map. The final groundwater potentiality zones are labeled into five ranks: very low (rank 1), low (rank 2), moderate (rank 3), high (rank 4), and very high (rank 5) ARPZs (Figure 16). The low to very low ARPZs occupied approximately 43% (4960.6 km²) of the studied region. In contrast, the moderate ARPZs occupied 15.2% (1760.6 km²). The rest, 41.8% (4835.3 km²) of the area, was inhabited by high and very high ARPZs (Figure 16). The findings show that the best ARPZs are concentrated in the southeastern, southwestern, and northeastern parts (Figure 16). It might be attributed to sedimentary succession-Quaternary alluvium deposits, suitable rainfall, good infiltration, high lineaments intensity, gentle slope, and sandy soil textures. On the other hand, steep slopes, very low NDVI, mostly nonfractured hard rocks (igneous, metamorphic, and carbonate rocks), clayey soil textures, high elevation, intrusive rocks, and low rainfall might be the reason behind lower ARPZs.

4.3. Verification

Without verification, the outputs from the final ARPZ would be impractical and ineffective. TDS (218–1528 ppm) and EC (451–2436 S/cm) concentrations decrease in the northeastern and northwestern regions (Figure 17a,b). They become more concentrated in the south and southwest, which can be attributed to seawater intrusion.

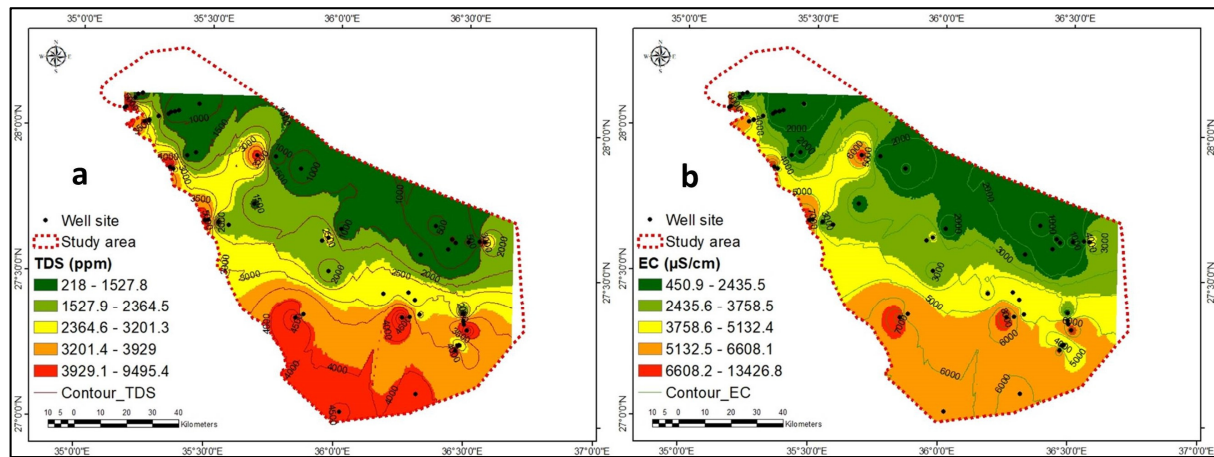


Figure 17. Verification of (a) TDS and (b) EC concentration of the Saq aquifer.

Barium and strontium concentrations increase in the southwest (Figure 18a,b), confirming seawater intrusion in that direction. The NO_3 concentration increases from 53 to 93 mg/L toward the center and northwest (Figure 18c), indicating that agricultural wastewater enters the aquifer system through the high porosity and permeability of the sedimentary and alluvium deposits. The NO_3 concentration decreases in the south, east, and southwest (0.18 mg/L) (Figure 18c). The hydrogeochemical data points are interpolated using ArcGIS's inverse distance weighted (IDW) method. The hydrogeochemical zonation ends at the borehole points, north section in Figures 17 and 18. Since there was no drilling data beyond that point, ArcGIS cannot contour and display a small white (empty) area.

Most of the low concentrations of NO_3 , TDS, and EC coincide with moderate to very high aquifer potentiality, indicating that the outputs are accurate. The correlation between high to very high aquifer potentiality and high aquifer TDS concentration has been attributed to seawater intrusion. Due to the high salinity of the groundwater in these regions, which precludes its use for agriculture and domestic purposes, exploration and exploitation of the aquifer have been neglected. Most drilled wells are in aquifers with high to very high potential, confirming the validity. They advocate for increased research and investment in agriculture and urbanization, particularly in this arid and coastal region. There is a strong correlation between zones of aquifer potentiality and low aquifer TDS concentration in aggregates from drilled wells. They validate the final ARPZ map and can add new wells to increase expenditures substantially. They increase per capita income, agriculture, urbanization, and the distribution of residents in rural, coastal, and urban zones, add new groundwater resources, decrease desalinated water, and encourage aquifer exploration and exploitation research. The Wadi Ad Disah springs (Figure 16) are located in a zone with a very high aquifer potentiality, which enhances the accuracy of the most promising investment areas. They discharged water with an EC of 420 to 740 $\mu\text{S}/\text{cm}$ from Paleozoic sandstone, which was considered excellent quality [20].

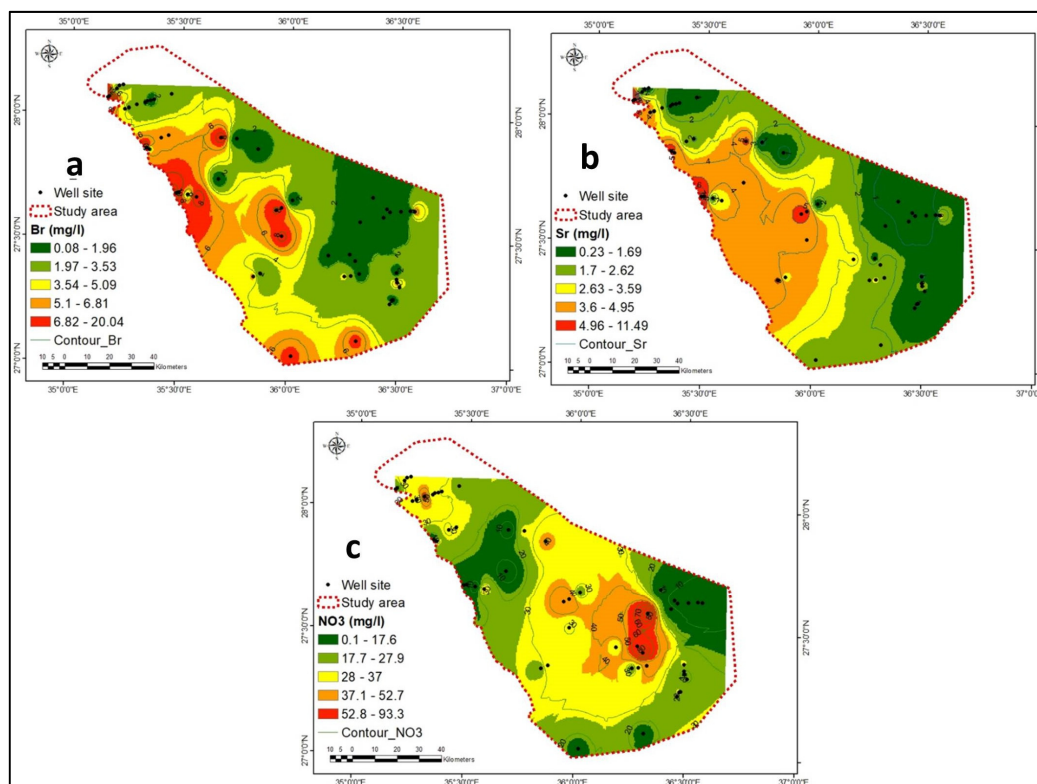


Figure 18. Verification of (a) Barium, (b) Sr, and (c) NO_3 content in the Saq aquifer.

5. Conclusions and Recommendations

The AHP, RS, and GIS techniques were applied to determine ARPZ in the Duba region of Tabuk province of SA's northwestern part to increase water resources and decrease the use of desalinated water (expensive). Groundwater potential zones were extracted using surface geology, rainfall, lineaments density, drainage density, slope, elevation, soil, and NDVI thematic layers. These parameters' input weights are determined by their contribution to aquifer potentiality and recharge. The investigation area is divided into five zones based on the aquifer potentiality map: very low, low, moderate, high, and very high potentiality. Low to very low aquifer potentiality is dispersed throughout the study area's western and central regions (43%). High to very high aquifer potentiality and recharge are primarily concentrated in the southeast, southwest, and northeast (41.8%), whereas the moderate zone accounts for 15.2% of the study area. High and very high aquifer potential coincides with drilled wells and low TDS and NO_3 concentrations in the Saq aquifer. The positive verification encourages the addition of new wells in high-potential investment zones. The ARPZ map provides new water resources for groundwater management and planning; they also increase agricultural, industrial, and domestic activity and the number of people who reside in a given area.

Supplementary Materials: The following supporting information can be downloaded at: <https://www.mdpi.com/article/10.3390/rs15102567/s1>, Table S1: Reference for calculation method in Table 1.

Author Contributions: Conceptualization, M.E. and M.Y.A.K.; methodology, M.E.; software, M.E.; verification, M.E.; writing—original draft preparation, M.Y.A.K. and M.E.; writing—review and editing, M.Y.A.K., J.C.E. and F.K.Z. All authors have read and agreed to the published version of the manuscript.

Funding: This research work was funded by Institutional Fund Projects under grant no. (IFPIP: 427-145-1443). Therefore, the authors gratefully acknowledge the technical and financial support provided by the Ministry of Education and King Abdulaziz University, DSR, Jeddah, Saudi Arabia.

Institutional Review Board Statement: Not applicable.

Informed Consent Statement: Not applicable.

Data Availability Statement: Not applicable.

Conflicts of Interest: The authors declare no conflict of interest.

References

1. Khan, M.Y.A.; ElKashouty, M.; Bob, M. Impact of rapid urbanization and tourism on the groundwater quality in Al Madinah city, Saudi Arabia: A monitoring and modeling approach. *Arab. J. Geosci.* **2020**, *13*, 922. [[CrossRef](#)]
2. Khan, M.Y.A.; El Kashouty, M.; Gusti, W.; Kumar, A.; Subyani, A.M.; Alshehri, A. Geo-Temporal Signatures of Physicochemical and Heavy Metals Pollution in Groundwater of Khulais Region—Makkah Province, Saudi Arabia. *Front. Environ. Sci.* **2022**, *9*, 699. [[CrossRef](#)]
3. Khan, M.Y.A.; ElKashouty, M.; Abdellattif, A.; Egbueri, J.C.; Taha, A.I.; Al Deep, M.; Shaaban, F. Influence of natural and anthropogenic factors on the hydrogeology and hydrogeochemistry of Wadi Itwad Aquifer, Saudi Arabia: Assessment using multivariate statistics and PMWIN simulation. *Ecol. Indic.* **2023**, 110287. [[CrossRef](#)]
4. Khan, M.Y.A.; Khan, B.; Chakrapani, G.J. Assessment of spatial variations in water quality of Garra River at Shahjahanpur, Ganga Basin, India. *Arab. J. Geosci.* **2016**, *9*, 516. [[CrossRef](#)]
5. Khan, M.Y.A.; Gani, K.M.; Chakrapani, G.J. Assessment of surface water quality and its spatial variation. A case study of Ramganga River, Ganga Basin, India. *Arab. J. Geosci.* **2016**, *9*, 28. [[CrossRef](#)]
6. Khan, M.Y.A.; Gani, K.M.; Chakrapani, G.J. Spatial and temporal variations of physicochemical and heavy metal pollution in Ramganga River—A tributary of River Ganges, India. *Environ. Earth Sci.* **2017**, *76*, 231. [[CrossRef](#)]
7. Khan, M.Y.A.; Hu, H.; Tian, F.; Wen, J. Monitoring the spatio-temporal impact of small tributaries on the hydrochemical characteristics of Ramganga River, Ganges Basin, India. *Int. J. River Basin Manag.* **2020**, *18*, 231–241. [[CrossRef](#)]
8. Panwar, S.; Yang, S.; Srivastava, P.; Khan, M.Y.A.; Sangode, S.J.; Chakrapani, G.J. Environmental magnetic characterization of the Alaknanda and Ramganga river sediments, Ganga basin, India. *Catena* **2020**, *190*, 104529. [[CrossRef](#)]
9. Yang, Y.; Liu, Y.; Yuan, Z.; Dai, J.; Zeng, Y.; Khan, M.Y.A. Analyzing the Water Pollution Control Cost-Sharing Mechanism in the Yellow River and Its Two Tributaries in the Context of Regional Differences. *Water* **2022**, *14*, 1678. [[CrossRef](#)]
10. Khan, M.Y.A.; Panwar, S.; Wen, J. Geochemistry of the dissolved load of the Ramganga River, Ganga Basin, India: Anthropogenic impacts and chemical weathering. *Front. Environ. Sci.* **2022**, *10*, 119. [[CrossRef](#)]
11. Gupta, M.K.; Kumar, R.; Banerjee, M.K.; Gupta, N.K.; Alam, T.; Eldin, S.M.; Khan, M.Y.A. Assessment of Chambal River Water Quality Parameters: A MATLAB Simulation Analysis. *Water* **2022**, *14*, 4040. [[CrossRef](#)]
12. Haq, M.A.; Khan, M.Y.A. Crop Water Requirements with Changing Climate in an Arid Region of Saudi Arabia. *Sustainability* **2022**, *14*, 13554. [[CrossRef](#)]
13. Agbasi, J.C.; Chukwu, C.N.; Nweke, N.D.; Uwajingba, H.C.; Khan, M.Y.A.; Egbueri, J.C. Water pollution indexing and health risk assessment due to PTE ingestion and dermal absorption for nine human populations in Southeast Nigeria. *Groundw. Sustain. Dev.* **2023**, *21*, 100921. [[CrossRef](#)]
14. Israil, M.; Al-Hadithi, M.; Singhal, D.C. Application of a resistivity survey and geographical information system (GIS) analysis for hydrogeological zoning of a piedmont area, Himalayan foothill region, India. *Hydrogeol. J.* **2006**, *14*, 753–759. [[CrossRef](#)]
15. Anbazhagan, S.; Ramasamy, S.M.; Edwin, J.M. Remote sensing and geophysical resistivity survey for groundwater exploration—A comparative analysis. In Proceedings of the Conference on Groundwater Exploration Techniques, Copenhagen, Denmark, 6–8 June 2000; pp. 177–181.
16. Vaux, H. Groundwater under stress: The importance of management. *Environ. Earth Sci.* **2011**, *62*, 19–23. [[CrossRef](#)]
17. Page, M.L.; Berjamy, B.; Fakir, Y.; Bourgin, F.; Jarlan, J.; Abourida, A.; Benrhanem, M.; Jacob, G.; Huber, M.; Sghrer, F.; et al. An integrated DSS for groundwater management based on remote sensing. The case of a semi-arid aquifer in Morocco. *Water Resour. Manag.* **2012**, *26*, 3209–3230. [[CrossRef](#)]
18. Adiat, K.; Nawawi, M.N.M.; Abdullah, K. Assessing the accuracy of GIS-based elementary multi criteria decision analysis as a spatial prediction tool—A case of predicting potential zones of sustainable groundwater resources. *J. Hydrol.* **2012**, *440*, 75–89. [[CrossRef](#)]
19. Manap, M.A.; Sulaiman, W.N.A.; Ramli, M.F.; Pradhan, B.; Surip, N. A knowledge-driven GIS modeling technique for groundwater potential mapping at the Upper Langat Basin, Malaysia. *Arab J. Geosci.* **2013**, *6*, 1621–1637. [[CrossRef](#)]
20. Machireddy, S.R. Delineation of groundwater potential zones in South East part of Anantapur District using remote sensing and GIS applications. *Sustain. Water Resour. Manag.* **2019**, *5*, 1695–1709. [[CrossRef](#)]
21. Jha, M.K.; Chowdary, V.M.; Chowdhury, A. Groundwater assessment in salboni block, West Bengal (India) using remote sensing, geographical information system and multi-criteria decision analysis techniques. *Hydrogeol. J.* **2010**, *18*, 1713–1728. [[CrossRef](#)]
22. Meijerink, A.M.J. Groundwater. In *Remote Sensing in Hydrology and Water Management*; Schultz, G.A., Engman, E.T., Eds.; Springer: Berlin/Heidelberg, Germany, 2000; pp. 305–325.
23. Machiwal, D.; Jha, M.K.; Mal, B.C. Assessment of groundwater potential in a semi-arid region of India using remote sensing, GIS and MCDM techniques. *Water Resour. Manag.* **2011**, *25*, 1359–1386. [[CrossRef](#)]

24. Waikar, M.L.; Nilawar, A.P. Identification of groundwater potential zone using remote sensing and GIS technique. *Int. J. Innov. Res. Sci. Eng. Technol.* **2014**, *3*, 12163–12174.
25. Echogdali, F.Z.; Boutaleb, S.; Bendarma, A.; Saidi, M.E.; Aadraoui, M.; Abioui, M.; Ouchchen, M.; Abdelrahman, K.; Fnais, M.S.; Sajinkumar, K.S. Application of analytical hierarchy process and geophysical method for groundwater potential mapping in the Tata basin, Morocco. *Water* **2022**, *14*, 2393. [[CrossRef](#)]
26. Saaty, T.L. *The Analytic Hierarchy Process: Planning, Priority Setting, Resource Allocation*; McGraw-Hill: New York, NY, USA, 1980.
27. Saranya, T.; Saravanan, S. Groundwater Potential Zone Mapping Using Analytical Hierarchy Process (Ahp) and Gis for Kancheepuram District, Tamilnadu, India. *Model. Earth Syst. Environ.* **2020**, *6*, 1105–1122. [[CrossRef](#)]
28. Kumar, A.; Krishna, A.P. Assessment of Groundwater Potential Zones in Coal Mining Impacted Hard-Rock Terrain of India by Integrating Geospatial and Analytic Hierarchy Process (Ahp) Approach. *Geocarto Int.* **2018**, *33*, 105–129. [[CrossRef](#)]
29. Ramanathan, R. A Note on the Use of the Analytic Hierarchy Process for Environmental Impact Assessment. *J. Environ. Manag.* **2001**, *63*, 27–35. [[CrossRef](#)]
30. Tesfamariam, S.; Sadiq, R. Risk-Based Environmental Decision-Making Using Fuzzy Analytic Hierarchy Process (F-Ahp). *Stoch. Environ. Res. Risk Assess.* **2006**, *21*, 35–50. [[CrossRef](#)]
31. Memarbashi, E.; Azadi, H.; Barati, A.A.; Mohajeri, F.; Van Passel, S.; Witlox, F. Land-Use Suitability in Northeast Iran: Application of Ahp-Gis Hybrid Model. *ISPRS Int. J. Geo-Inf.* **2017**, *6*, 396. [[CrossRef](#)]
32. Contreras, F.; Hanaki, K.; Aramaki, T.; Connors, S. Application of Analytical Hierarchy Process to Analyze Stakeholders Preferences for Municipal Solid Waste Management Plans, Boston, USA. *Resour. Conserv. Recycl.* **2008**, *52*, 979–991. [[CrossRef](#)]
33. Khoshand, A.; Kamalan, H.; Rezaei, H. Application of Analytical Hierarchy Process (Ahp) to Assess Options of Energy Recovery from Municipal Solid Waste: A Case Study in Tehran, Iran. *J. Mater. Cycles Waste Manag.* **2018**, *20*, 1689–1700. [[CrossRef](#)]
34. Abrams, W.; Ghoneim, E.; Shew, R.; LaMaskin, T.; Al-Bloushi, K.; Hussein, S.; AbuBakr, M.; Al-Mulla, E.; Al-Awar, M.; El-Baz, F. Delineation of groundwater potential (GWP) in the northern United Arab Emirates and Oman using geospatial technologies in conjunction with Simple Additive Weight (SAW), Analytical Hierarchy Process (AHP), and Probabilistic Frequency Ratio (PFR) techniques. *J. Arid Environ.* **2018**, *157*, 77–96. [[CrossRef](#)]
35. Rajasekhar, M.; Raju, G.S.; Sreenivasulu, Y.; Raju, R.S. Delineation of groundwater potential zones in semi-arid region of Jilledubanderu river basin, Anantapur District, Andhra Pradesh, India using fuzzy logic, AHP and integrated fuzzy-AHP approaches. *HydroResearch* **2019**, *2*, 97–108. [[CrossRef](#)]
36. Dar, T.; Rai, N.; Bhat, A. Delineation of potential groundwater recharge zones using analytical hierarchy process (AHP). *Geol. Ecol. Landsc.* **2021**, *5*, 292–307. [[CrossRef](#)]
37. Khan, M.Y.A.; ElKashouty, M.; Tian, F. Mapping Groundwater Potential Zones Using Analytical Hierarchical Process and Multicriteria Evaluation in the Central Eastern Desert, Egypt. *Water* **2022**, *14*, 1041. [[CrossRef](#)]
38. Radulović, M.; Brdar, S.; Mesaroš, M.; Lukić, T.; Savić, S.; Basarin, B.; Crnojević, V.; Pavić, D. Assessment of Groundwater Potential Zones Using GIS and Fuzzy AHP Techniques—A Case Study of the Titel Municipality (Northern Serbia). *ISPRS Int. J. Geo-Inf.* **2022**, *11*, 257. [[CrossRef](#)]
39. Khan, M.Y.A.; ElKashouty, M.; Subyani, A.M.; Tian, F.; Gusti, W. GIS and RS intelligence in delineating the groundwater potential zones in Arid Regions: A case study of southern Aseer, southwestern Saudi Arabia. *Appl. Water Sci.* **2022**, *12*, 3. [[CrossRef](#)]
40. Ikirri, M.; Boutaleb, S.; Ibraheem, I.M.; Abioui, M.; Echogdali, F.Z.; Abdelrahman, K.; Id-Belqas, M.; Abu-Alam, T.; El Ayady, H.; Essoussi, S.; et al. Delineation of Groundwater Potential Area using an AHP, Remote Sensing, and GIS Techniques in the Ifni Basin, Western Anti-Atlas, Morocco. *Water* **2023**, *15*, 1436. [[CrossRef](#)]
41. Arumugam, M.; Kulandaisamy, P.; Karthikeyan, S.; Thangaraj, K.; Senapathi, V.; Chung, S.Y.; Muthuramalingam, S.; Rajendran, M.; Sugumaran, S.; Manimuthu, S. An Assessment of Geospatial Analysis Combined with AHP Techniques to Identify Groundwater Potential Zones in the Pudukkottai District, Tamil Nadu, India. *Water* **2023**, *15*, 1101. [[CrossRef](#)]
42. World Bank. *A Water Sector Assessment Report on Countries of the Cooperation Council of the Arab State of the Gulf*; Report No. 32539-MNA; World Bank: Washington, DC, USA, 2005.
43. FAO/WHO Expert Committee on Food Additives; Food and Agriculture Organization; World Health Organization. *Safety Evaluation of Certain Food Additives (No. 56)*; World Health Organization: Geneva, Switzerland, 2006.
44. Al-Rashed, M.F.; Sherif, M.M. Water resources in the GCC countries: An overview. *Water Resour. Manag.* **2000**, *14*, 59–75. [[CrossRef](#)]
45. Mallick, J.; Singh, C.K.; AlMesfer, M.K.; Kumar, A.; Khan, R.A.; Islam, S.; Rahman, A. Hydro-Geochemical Assessment of Groundwater Quality in Aseer Region, Saudi Arabia. *Water* **2018**, *10*, 1847. [[CrossRef](#)]
46. Al-Laboun, A.A. Stratigraphy and hydrocarbon potential of the Paleozoic succession in both Tabuk and Widyan basins, Arabia. *AAPG* **1986**, 373–397.
47. Alamrani, N.A.; Almutairi, F.M.; Alatawi, N.M.; Mogharbel, A.T.; Al-Aoh, H.A.; Hajri, A.K.; Keshk, A.A. and Elsayed, N.H. Assessment and management of heavy metals pollution in Tabuk region Saudi Arabia, improvement for future development: A review. *Wulfenia* **2022**, *29*, 32–51.
48. AQUASTAT Survey. *Irrigation in the Middle East Region in Figures*; AQUASTAT: North Somerset, UK, 2008; pp. 1–13.
49. Yahiaoui, B.; Agoubi, B.; Kharroubi, A. Groundwater potential recharge areas delineation using groundwater potential recharge index (GPRI) within arid areas: Ghomrassen, south Tunisia. *Arab. J. Geosci.* **2021**, *14*, 919. [[CrossRef](#)]

50. Prasad, R.K.; Mondal, N.C.; Banerjee, P.; Nandakumar, M.V.; Singh, V.S. Deciphering potential groundwater zone in hardrock through the application of GIS. *Environ. Geol.* **2008**, *55*, 467–475. [CrossRef]
51. Das, B.; Pal, S.C. Assessment of groundwater recharge and its potential zone identification in groundwater-stressed Goghat-I block of Hugli District, West Bengal, India. *Environ. Dev. Sustain.* **2019**, *22*, 5905–5923. [CrossRef]
52. Rajesh, J.; Pande, C.; Kadam, S.A.; Gorantiwar, S.D.; Shinde, M.G. Exploration of groundwater potential zones using analytical hierarchical process (AHP) approach in the Godavari river basin of Maharashtra in India. *Appl. Water Sci.* **2021**, *11*, 182. [CrossRef]
53. GASTAT. General Authority for Statistics. 2016. Available online: <http://www.stats.gov.sa/en> (accessed on 13 February 2023).
54. MEWA. Ministry of Environment, Water and Agriculture. 2016. Available online: <https://www.mewa.gov.sa/en/Pages/default.aspx> (accessed on 14 January 2023).
55. Ouda, O. Water demand versus supply in Saudi Arabia: Current and future challenges. *Int. J. Water Resour. Dev.* **2014**, *30*, 335–344. [CrossRef]
56. Al-Omran, A.M.; Aly, A.A.; Al-Wabel, M.I.; Sallam, A.S.; Al-Shayaa, M.S. Hydrochemical characterization of groundwater under agricultural land in arid environment: A case study of Al-Kharj, Saudi Arabia. *Arab. J. Geosci.* **2016**, *9*, 68. [CrossRef]
57. Ali, I.; Hasan, M.A.; Alharbi, O.M.L. Toxic metal ions contamination in the groundwater, Kingdom of Saudi Arabia. *J. Taibah Univ. Sci.* **2020**, *14*, 1571–1579. [CrossRef]
58. Mallick, J.; Singh, C.K.; AlMesfer, M.K.; Singh, P.V.; Alsubih, M. Groundwater Quality Studies in the Kingdom of Saudi Arabia: Prevalent Research and Management Dimensions. *Water* **2021**, *13*, 1266. [CrossRef]
59. Hikal, W.M.; Al Hawiti, A.K.; Atawi, M.M.A.; MF, M.; Al Qahtani, F.S.; Al Balawi, A.S. Determination of Iron in some Fish Species from the Red Sea, Duba Coast, Tabuk, Saudi Arabia. *International Journal of Healthcare Sciences* **2019**, *7*, 298–308.
60. MWE. Supporting Documents for King Hassan II Great Water Prize. 2012. Available online: http://www.worldwatercouncil.org/fileadmin/www/Prizes/Hassan_II/Candidates_2011/16.Ministry_ (accessed on 30 November 2012).
61. Alsaleh, M. Natural springs in northwest Saudi Arabia. *Arab. J. Geosci.* **2017**, *10*, 335. [CrossRef]
62. Alhumimidi, M.S. An integrated approach for identification of seawater intrusion in coastal region: A case study of northwestern Saudi Arabia. *J. King Saud Univ.—Sci.* **2020**, *32*, 3187–3194. [CrossRef]
63. Jerais, A.A. Hydrogeology of Saq Aquifer in Hail Region. Master’s Thesis, Faculty of Earth Sciences, King Abdulaziz University, Jeddah, Saudi Arabia, 1986.
64. Al-Ahmadi, M.E. Hydrogeology of the Saq Aquifer Northwest of Tabuk, Northern Saudi Arabia. *Earth Sci.* **2007**, *20*, 51–66. [CrossRef]
65. King Fahd University Staff. *Groundwater Resources Evaluation in Saudi Arabia and Long-term Strategic Plan for Fresh Groundwater Use, King Fahd University Petroleum and Minerals*; KFUPM Press: Dhahran, Saudi Arabia, 1987; 168p.
66. Edgell, H.S. Aquifers of Saudi Arabia and their Geological Framework. *Arab. J. Sci. Eng.* **1997**, *22*, 5–31.
67. Krishnamurthy, J.; Kumar, N.V.; Jayaraman, V.; Manivel, M. An approach to demarcate ground water potential zones through remote sensing and a geographical information system. *Int. J. Remote Sens.* **1996**, *17*, 1867–1884. [CrossRef]
68. Saraf, A.K.; Choudhury, P.R. Integrated remote sensing and GIS for groundwater exploration and identification of artificial recharge sites. *Int. J. Remote Sens.* **1998**, *19*, 1825–1841. [CrossRef]
69. Butler, M.; Wallace, J.; Lowe, M. Groundwater quality classification using GIS contouring methods for cedar valley, Iron County, Utah. *Digit. Mapp. Technol.* **2002**, *2002*, 207.
70. Asadi, S.S.; Vuppala, P.; Reddy, M.A. Remote sensing and GIS techniques for evaluation of groundwater quality in municipal corporation of Hyderabad (Zone-V), India. *Int. J. Environ. Res. Public Health* **2007**, *4*, 45–52. [CrossRef]
71. Yammani, S. Groundwater quality suitable zones identification: Application of GIS, Chittoor area, Andhra Pradesh, India. *Environ. Geol.* **2007**, *53*, 201–210. [CrossRef]
72. Roy, S.; Hazra, S.; Chanda, A.; Das, S. Assessment of groundwater potential zones using multi-criteria decision-making technique: A micro-level case study from red and lateritic zone (RLZ) of West Bengal, India. *Sustain. Water Resour. Manag.* **2020**, *6*, 4. [CrossRef]
73. Arefin, R. Groundwater potential zone identification at Plio-Pleistocene elevated tract, Bangladesh: AHP-GIS and remote sensing approach. *Groundw. Sustain. Dev.* **2020**, *10*, 100340. [CrossRef]
74. Patra, S.; Mishra, P.; Mahapatra, S.C. Delineation of groundwater potential zone for sustainable development: A case study from Ganga Alluvial Plain covering Hooghly district of India using remote sensing, geographic information system and analytic hierarchy process. *J. Clean Prod.* **2018**, *172*, 2485–2502. [CrossRef]
75. Biswas, S.; Mukhopadhyay, B.P.; Bera, A. Delineating groundwater potential zones of agriculture dominated landscapes using GIS based AHP techniques: A case study from Uttar Dinajpur district, West Bengal. *Environ. Earth Sci.* **2020**, *79*, 302. [CrossRef]
76. Kadam, A.K.; Umrikar, B.N.; Sankhua, R.N. Assessment of recharge potential zones for groundwater development and management using geospatial and MCDA technologies in semiarid region of Western India. *Appl. Water Sci.* **2020**, *2*, 312. [CrossRef]
77. Srivastava, P.K.; Bhattacharya, A.K. Groundwater assessment through an integrated approach using remote sensing, GIS and resistivity techniques: A case study from a hard rock terrain. *Int. J. Remote Sens.* **2006**, *27*, 4599–4620. [CrossRef]
78. Das, S.; Behera, S.C.; Kar, A.; Narendra, P.; Guha, S. Hydrogeomorphological mapping in groundwater exploration using remotely sensed data—A case study in keonjhar district, orissa. *J. Ind. Soc. Remote Sens.* **1997**, *25*, 247–259. [CrossRef]
79. Hardcastle, K.C. Photolineament factor: A new computer-aided method for remotely sensing the degree to which bedrock is fractured. *Photogramm. Eng. Remote Sens.* **1995**, *61*, 739–746.

80. Devi, S.P.; Srinivasulu, S.; Raju, K.K. Delineation of groundwater potential zones and electrical resistivity studies for groundwater exploration. *Environ. Geol.* **2001**, *40*, 1252–1264. [[CrossRef](#)]
81. Magowe, M.; Carr, J.R. Relationship between lineaments and groundwater occurrence in western Botswana. *Groundwater* **1999**, *37*, 282–286. [[CrossRef](#)]
82. Rao, N.S.; Chakradhar, G.K.J.; Srinivas, V. Identification of groundwater potential zones using remote sensing techniques in and around Guntur town, Andhra Pradesh, India. *J. Indian Soc. Remote Sens.* **2001**, *29*, 69. [[CrossRef](#)]
83. Razandi, Y.; Pourghasemi, H.R.; Neisani, N.S.; Rahmati, O. Application of analytical hierarchy process, frequency ratio, and certainty factor models for groundwater potential mapping using GIS. *Earth Sci. Inform.* **2015**, *8*, 867–883. [[CrossRef](#)]
84. Abijith, D.; Saravanan, S.; Singh, L.; Jennifer, J.J.; Saranya, T.; Parthasarathy, K.S.S. GIS-based multi-criteria analysis for identification of potential groundwater recharge zones—A case study from Ponnaniyar watershed, Tamil Nadu, India. *HydroResearch* **2020**, *3*, 1–14. [[CrossRef](#)]
85. Das, N.; Mukhopadhyay, S. Application of multi-criteria decision making technique for the assessment of groundwater potential zones: A study on Birbhum district, West Bengal, India. *Environ. Dev. Sustain.* **2018**, *22*, 931–955. [[CrossRef](#)]
86. Nithya, C.N.; Srinivas, Y.; Magesh, N.S.; Kaliraj, S. Assessment of groundwater potential zones in Chittar basin, Southern India using GIS based AHP technique. *Remote Sens. Appl. Soc. Environ.* **2019**, *15*, 100248. [[CrossRef](#)]
87. Godebo, T.R. Application of Remote Sensing and GIS for Geological Investigation and Groundwater Potential Zone Identification, Southeastern Ethiopian Plateau, Bale Mountains and the Surrounding Areas. Ph.D. Thesis, Addis Ababa University, Addis Ababa, Ethiopia, 2005.
88. Doll, P.; Fiedler, K. Global-scale modeling of groundwater recharge. *Hydrol. Earth Syst. Sci.* **2008**, *12*, 863–885. [[CrossRef](#)]

Disclaimer/Publisher’s Note: The statements, opinions and data contained in all publications are solely those of the individual author(s) and contributor(s) and not of MDPI and/or the editor(s). MDPI and/or the editor(s) disclaim responsibility for any injury to people or property resulting from any ideas, methods, instructions or products referred to in the content.